

A STUDY OF B-TYPE STARS

A Thesis submitted to the  
University of Edinburgh  
for the degree of

MASTER OF SCIENCE

by

BRUCE N. G. GUTHRIE, B.Sc. (St. Andrews)

JUNE, 1964.



## ABSTRACT

The effect of rotation on quantities used in classifying B-type stars is discussed. The tendency for stars with high rotational velocities to have weaker Balmer lines for the same  $(U - B)_0$  has been investigated using published data. Abt's explanation of the effect in terms of the change in effective surface gravity due to rotation is confirmed. A correction term in Crawford's method of determining ages of clusters and field stars from Balmer line intensities and UBV photometry is derived. It is shown that errors in age determinations due to rotation are much smaller when the wavelength  $\lambda_1$  of the Balmer discontinuity is used instead of Balmer line intensities. A colour index sensitive to  $\lambda_1$  is discussed. Methods of determining the inclinations of the axes of rotation are suggested. It is shown that the "cosmic dispersion" in the relation between Balmer line intensities and absolute magnitudes is largely caused by rotation. A scheme of two-dimensional spectral classification using measurements of the position and size of the Balmer discontinuity on low dispersion objective prism plates is outlined. Rotational velocities for 18 stars have been derived from slit spectrograms; several lines including five Balmer lines were measured for each star.

CONTENTS

	Page
Chapter 1    Introduction . . . . .	1
Chapter 2    The effect of rotation on Balmer line intensities . . . . .	5
Chapter 3    Spectral classification at low dispersion . . . . .	30
Chapter 4    Measurement of rotational velocities . . . . .	45
Chapter 5    Ages and distances of B-type stars . . . . .	61
Conclusions . . . . .	91
Acknowledgements . . . . .	94
References . . . . .	95

## CHAPTER 1

### INTRODUCTION

The importance of B-type stars in galactic research lies in their high luminosity, which allows them to be observed to greater distances than for stars of later types for a given apparent magnitude. They are concentrated towards the galactic plane, and many are members of OB associations. They are useful in investigations of the distribution of interstellar matter, since colour excesses may be determined for them directly from UBV photometry. In order to take advantage of these intrinsic properties of B-type stars, absolute magnitudes must be known so that the distances of the stars may be found.

The determination of absolute magnitudes is performed in two stages. First, a suitable quantity sensitive to luminosity must be chosen and methods developed for measuring this quantity. Secondly, this observed quantity must be calibrated against absolute magnitude using nearby stars whose absolute magnitudes may be determined by direct methods such as the measurement of trigonometric parallaxes.

For B-type stars the equivalent widths of the Balmer lines are the most suitable quantities for determining absolute magnitudes. The

Balmer lines are broadened by the Stark effect which is sensitive to pressure. Consequently they are much broader in dwarfs than in supergiants.

Equivalent widths of Balmer lines have been measured photographically from slit spectrograms by Petrie (1952) and Sinnerstad (1961) for calibration against absolute magnitudes. This method of measuring equivalent widths is subject to errors in determining the characteristic curve for each plate and in drawing the continuum. It may be applied only to fairly bright stars, and the labour involved in obtaining and reducing each spectrogram is considerable. There is, however, the advantage that spectral classification and radial velocities may be obtained from the same spectrograms.

A more rapid and accurate method of measuring Balmer line intensities was introduced by Ström<sup>g</sup>ren (1952), who used interference filters, including one centred on the H $\beta$  line, for narrow-band photoelectric photometry. Crawford (1958) made extensive observations on B-type stars with a photoelectric photometer which had a beam-splitter and two photomultipliers for simultaneous observation of the H $\beta$  line through interference filters with half-widths of 15 and 150Å. A filter-slide arrangement made it possible to alternate between the 15Å H $\beta$  filter and another 150Å H $\beta$  filter, so that the relative sensitivity of the two photomultipliers

could be determined for each star observed. The index

$$\beta = 2.5 \left[ \log I(150\text{A filter}) - \log I(15\text{A filter}) \right] + \text{constant},$$

where  $I(150\text{A filter})$  and  $I(15\text{A filter})$  denote the measured intensities through the 150 and 15A filters respectively, is a measure of the intensity of the  $H\beta$  line. Crawford showed that his  $\beta$  measures together with measures of the intrinsic colour-index  $(U - B)_0$  derived from UBV photometry gave a two-dimensional classification of B-type stars, and that the positions of stars in the  $\beta - (U - B)_0$  diagram were correlated with the relative ages of the stars. For a given telescope aperture and exposure time, observable stars for photoelectric photometry with interference filters are several magnitudes fainter than those for which slit spectrograms may be obtained.

B-type stars are too distant for trigonometric parallaxes to be used in the calibration of absolute magnitudes. Absolute magnitudes for B-type members of the II Sco association have been determined by Bertiau (1958) from proper motions and radial velocities. Alternatively, the main sequences of clusters containing B-type stars may be fitted to that of the Hyades, for which Heckmann and Lübeck (1956) determined absolute magnitudes from proper motions.

The behaviour of the spectral lines in B-type stars has been studied by Williams (1936), Sinnerstad (1961), and in a series of investigations at the Royal Observatory, Edinburgh. The HeI and CII lines have maximum



intensities at spectral type B2. The intensities of the MgII 4481 line and the SiII 4128-4130 blend increase toward the later B-types. Lines of OII, NiII and SiIV are present in only the earliest of B-type stars. The spectral lines apart from those of hydrogen and HeI show a tendency to be stronger in supergiants than in dwarfs.

B-type stars are the most suitable stars for investigating the interstellar bands (e.g. the band at 4430A) whose origin is unknown. Their profiles are most easily studied in the spectra of these stars, since the bands are blended with fewer stellar lines than in late-type stars. More distant stars are within reach of observation owing to the high luminosity of B-type stars.

An outstanding feature of early-type stars is their rapid rotation. For main sequence B-type stars the average value of the equatorial rotational velocity is about 200 km/sec (Slettebak and Howard, 1955). This is sufficient to produce a considerable distortion in the shape of the star, and its effect on quantities used in spectral classification should therefore be examined.

## CHAPTER 2

### THE EFFECT OF ROTATION ON BALMER LINE INTENSITIES

#### Introduction

While studying the rotational velocities of stars in the Orion association, McNamara and Larsson (1962) noted that on the plot of the intensity  $\beta$  of the  $H\beta$  line against  $(U - B)_0$  the stars with large rotational velocities showed a tendency to have smaller values of  $\beta$  than those with small rotational velocities. McNamara (1962) confirmed the effect using rotational velocities for stars in the  $\alpha$  Persei and I Lac associations and additional stars in the Orion association measured by Abt and Hunter (1962).

Since this will affect determinations of absolute magnitude  $M_v$  from Balmer line intensities and of the ages of stars and clusters from their positions on the  $\beta - (U - B)_0$  diagram, a more detailed investigation is called for. It may also be possible from UBV photometry and Balmer line intensities to estimate the approximate inclinations of the axes of rotation of some early-type cluster members.

#### Selection of stars for discussion

Crawford (1958) showed that luminosity class III stars lie above the main sequence on the  $\beta - (U - B)_0$  diagram, and therefore a luminosity class III star with low rotational velocity might be in the same position



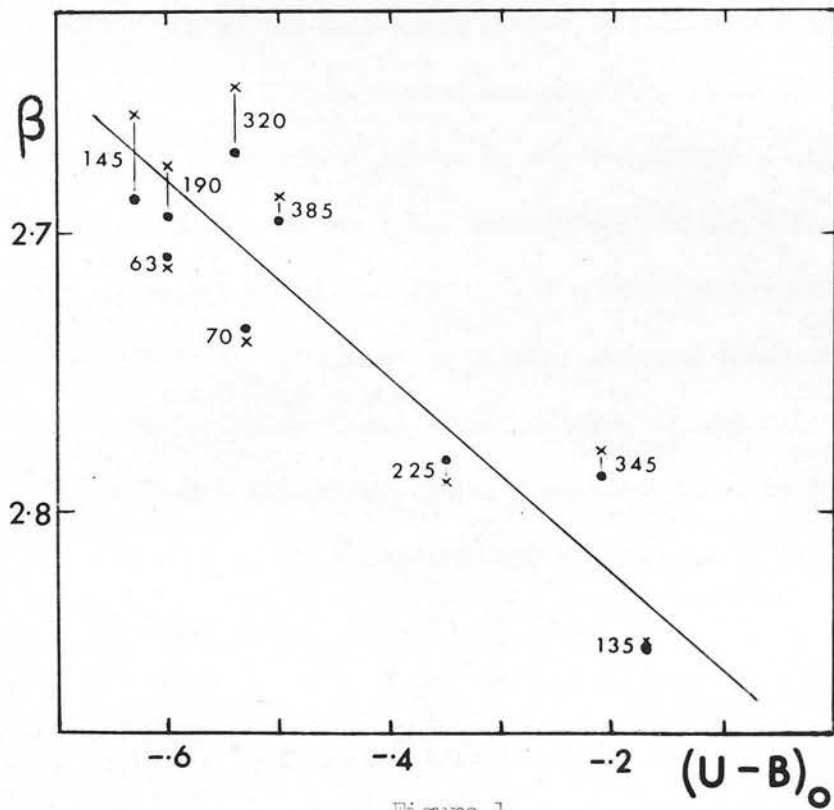


Figure 1

$\beta - (U - B)_0$  DIAGRAM FOR THE  $\alpha$  PERSEI CLUSTER.

FILLED CIRCLES DENOTE  $\beta$  VALUES, AND

CROSSES DENOTE TRANSFORMED  $\Gamma$  VALUES.

as a luminosity class V star with high rotational velocity. Hence only luminosity class V stars are considered. The discussion is also limited to stars earlier than A0 for which the nomogram by Johnson (1958) can be used for finding  $(U - B)_0$ . Stars with spectral peculiarities or binary characteristics such as line structure are omitted.

#### The cause of the effect

Since the half-width of the  $H\beta$  filter used by Crawford (1958) for clusters and associations was only 15A, it is first necessary to decide whether the effect is due to the broadening of the line by rotation or to a change in its total absorption. If the effect is due to broadening, it should be smaller for measures taken with a filter with greater half-width. Bappu et al. (1962) obtained intensities  $\Gamma$  of the  $H\gamma$  line using a filter of half-width 45A for several clusters including the  $\alpha$  Persei cluster for which  $\beta$  measures taken by Crawford (1958) are also available. The  $\Gamma$  measures may be transformed to Crawford's system using the relation

$$\beta = 3.1658 - 0.00227 \Gamma \quad (1)$$

given by Bappu et al. (1962). The  $\beta$  and transformed  $\Gamma$  measures are plotted against  $(U - B)_0$  in Fig. 1.  $(U - B)_0$  is obtained from the UBV photometry by Mitchell (1960) using Johnson's nomogram. The deviations  $\delta\beta$  and  $\delta(\text{transformed } \Gamma)$  from the line in Fig. 1 are plotted in Fig. 2 against the rotational velocity  $v_{\text{ini}}$ , the mean of the values given by Abt and Hunter (1962) and Slettebak and Howard (1955) being taken.

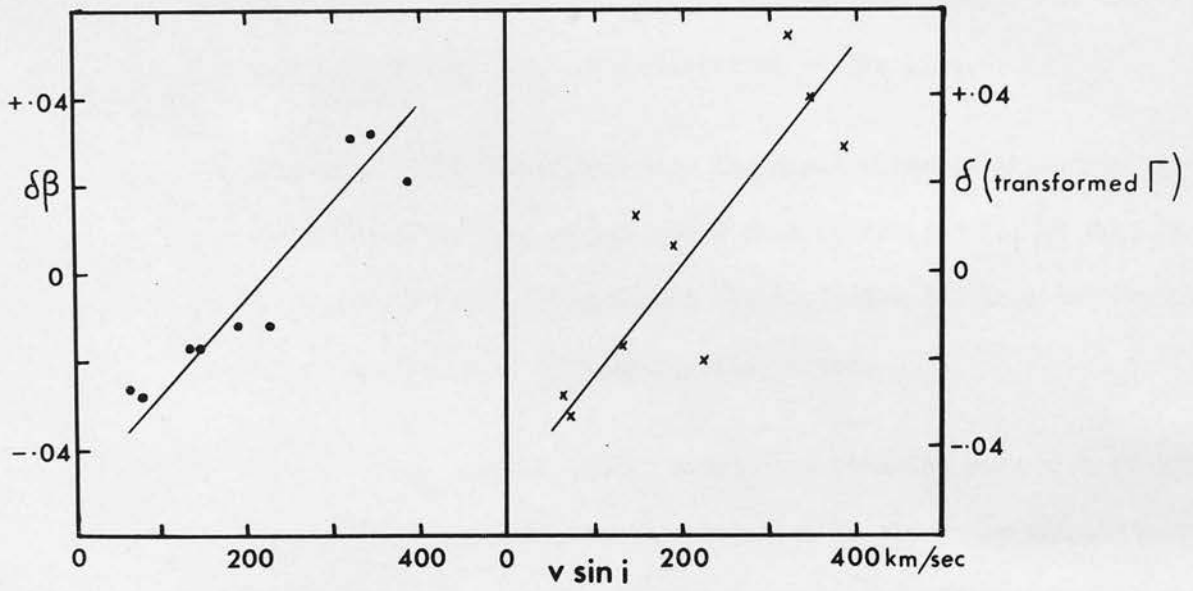


Figure 2

DEVIATIONS IN  $\beta$  AND TRANSFORMED  $\Gamma$  FOR THE  $\alpha$  PERSEI CLUSTER.

There is an approximately linear relation between the deviations and  $v \sin i$  in each case. The slope is  $0.00022 \pm 0.00004$  in  $\beta$  per km/sec in  $v \sin i$  for the  $\beta$  measures, and  $0.00025 \pm 0.00005$  in  $\beta$  per km/sec in  $v \sin i$  for the transformed  $\Gamma$  measures. This shows that the effect is not significantly different when a filter with a larger half-width is used, and therefore rotation must change the total absorption of the line.

McNamara (1962) suggested that incipient emission might be the cause and pointed out that the effect would then be smaller for H $\gamma$  than for H $\beta$ . The above analysis for the  $\alpha$  Persei cluster rules out this possibility except perhaps for very rapidly rotating stars.

McNamara and Larsson (1962) noted that binaries were more frequent among stars with high rotational velocities in the Orion association and suggested this as a possible cause. However, the effect is still present in the Pleiades and the  $\alpha$  Persei clusters even when suspected binaries are eliminated. McNamara (1963) also points out that known binaries in the II Sco association do not deviate significantly from the mean  $\beta - (U - B)_0$  relation.

The true explanation is probably that the rotation lowers the effective surface gravity of the equatorial region of the star, as suggested by Abt (McNamara and Larsson, 1962). The observed effect will, of course, be smaller, since the line intensities refer to the entire surface of the star and not only the equatorial region. An analysis of

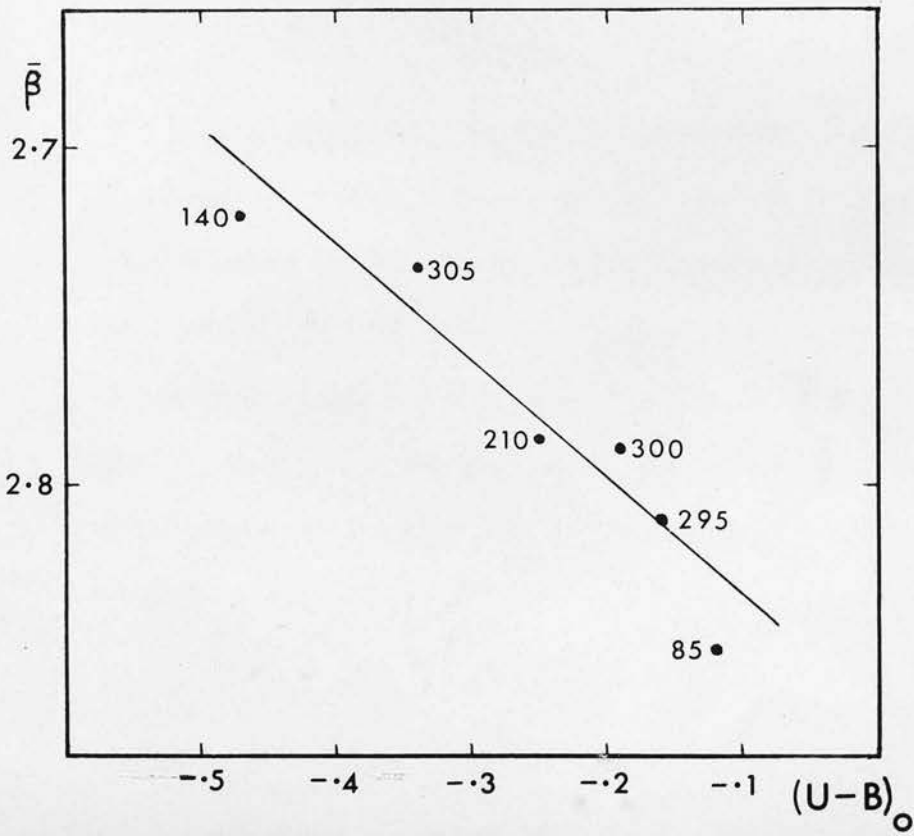


Figure 3

$\bar{\beta} - (U - B)_0$  DIAGRAM FOR THE PLEIADES.

the effect of rotation on the position of a star in the H-R diagram has been carried out by Sweet and Roy (1953), and their results are used later in this chapter to show that Abt's explanation gives the correct order of magnitude for the effect.

#### Analysis of clusters and associations

In order to examine the effect in more detail, consideration has been to the following clusters and associations for which the necessary observations are available.

(i) Pleiades.  $(U - B)_0$  has been determined from the UBV photometry by Johnson and Morgan (1953). The mean value  $\bar{\beta}$  of Crawford's  $\beta$  measures and  $\Gamma$  measures by Bappu et al. (1962) transformed to Crawford's system by equation (1) has been taken. The values of  $v \sin i$  are the means of those by Slettebak (1954) and Abt and Hunter (1962).  $\bar{\beta}$  has been plotted against  $(U - B)_0$  in Fig. 3. The plot of the deviations  $\delta\bar{\beta}$  from the line in Fig. 3 against  $v \sin i$  is given in Fig. 4. The slope is 0.00016 in  $\beta$  per km/sec in  $v \sin i$ .



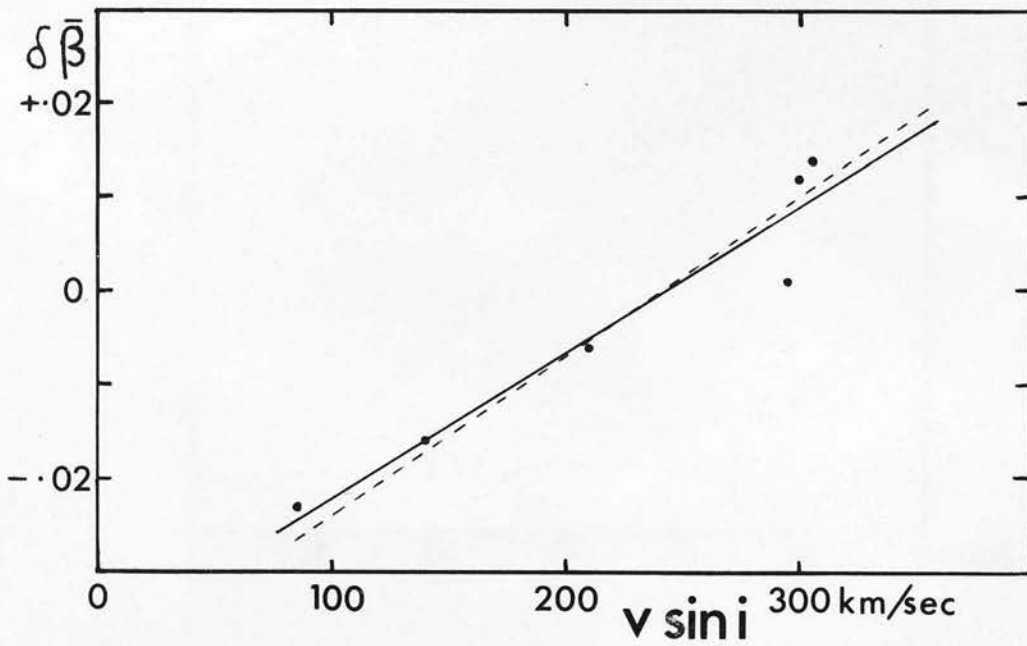


Figure 4  
DEVIATIONS IN  $\bar{\beta}$  FOR THE PLEIADES.

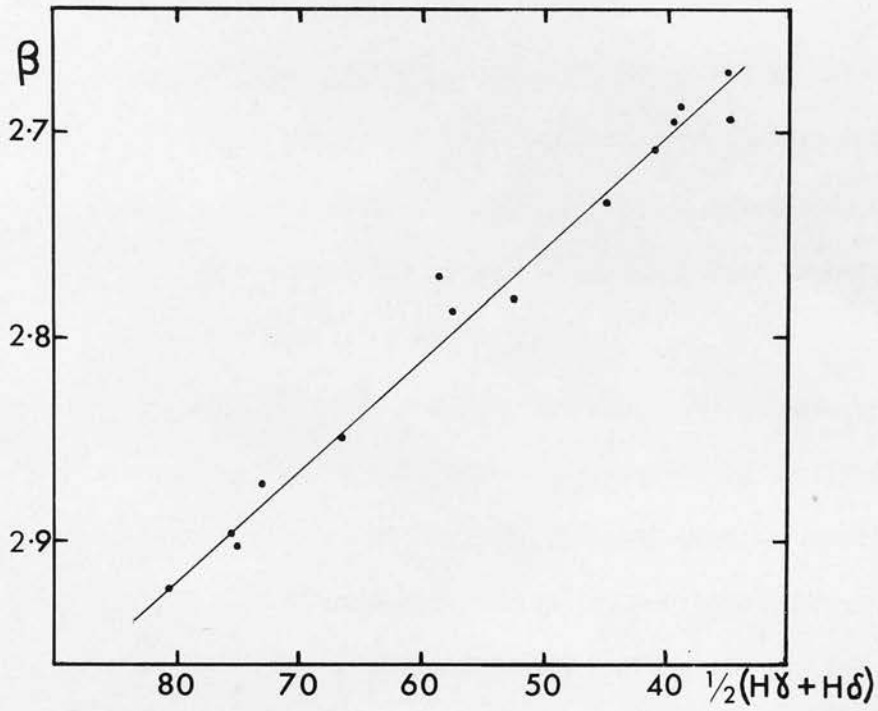


Figure 5

TRANSFORMATION BETWEEN  $\beta$  AND  $\frac{1}{2}(H\gamma + H\delta)$  FOR LUMINOSITY CLASS V STARS IN THE  $\alpha$  PERSEI CLUSTER.

Table 1

## PLEIADES

HD	Hertzsprung		(U - B) <sub>0</sub>	$\beta$	Transformed		vsini
	No.	MK			$\Gamma$	$\bar{\beta}$	
23338	156	B6 V	-.47	2.716	2.723	2.720	140
23432	255	B8 V	-.25	2.790	2.782	2.786	210
23441	265	B9 V	-.16		2.810	2.810	295
23753	722	B8 V	-.34		2.735	2.735	305
23873	910	B9.5 V	-.12		2.848	2.848	85
23923	977	B9 V	-.19		2.789	2.789	300

(ii)  $\alpha$  Persei cluster. The UBV photometry by Mitchell (1960) has been used. HY and H $\delta$  have been measured photographically by Ljunggren and Oja (1961) on objective prism spectra using a photometer with a slit width of 25A at HY. These have been transformed to Crawford's system using the relation

$$\beta = 2.478 + 0.00552 \frac{1}{2}(HY + H\delta) \quad (2)$$

derived from Fig. 5. The mean of  $\beta$  measures by Crawford (1958),  $\Gamma$  measures by Bappu et al. (1962) transformed by equation (1) and  $\frac{1}{2}(HY + H\delta)$  transformed by equation (2) has been taken. Proceeding in the same way as for the Pleiades, the slope for the deviations has been derived from Figs. 6 and 7 and is 0.00019 in  $\beta$  per km/sec in vsini.

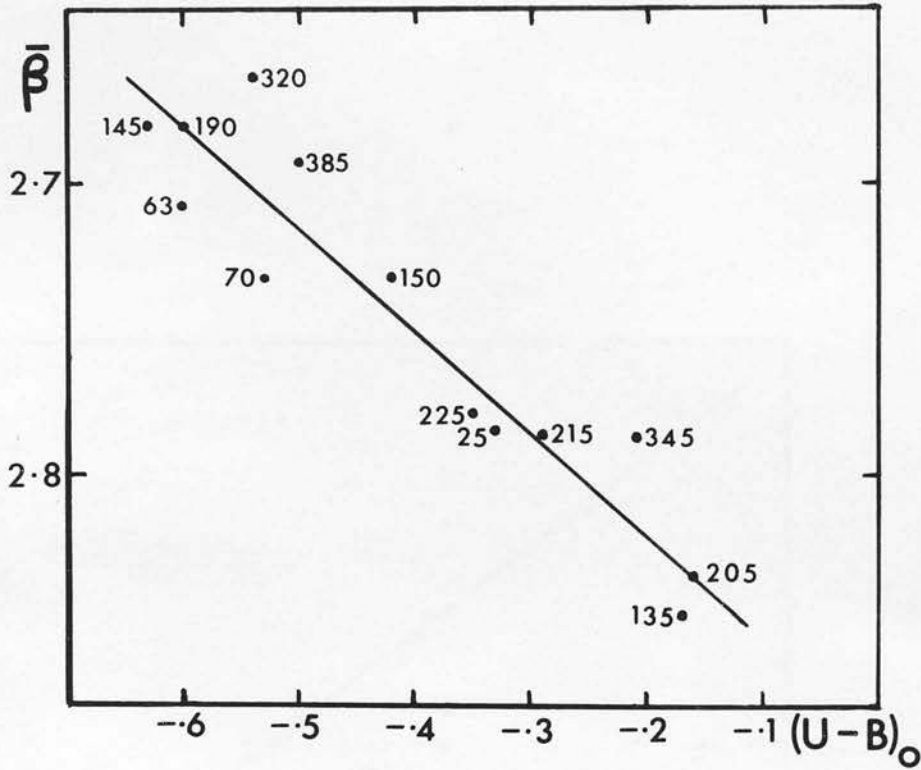


Figure 6

$\bar{\rho} - (U - B)_0$  DIAGRAM FOR THE  $\alpha$  PERSEI CLUSTER.

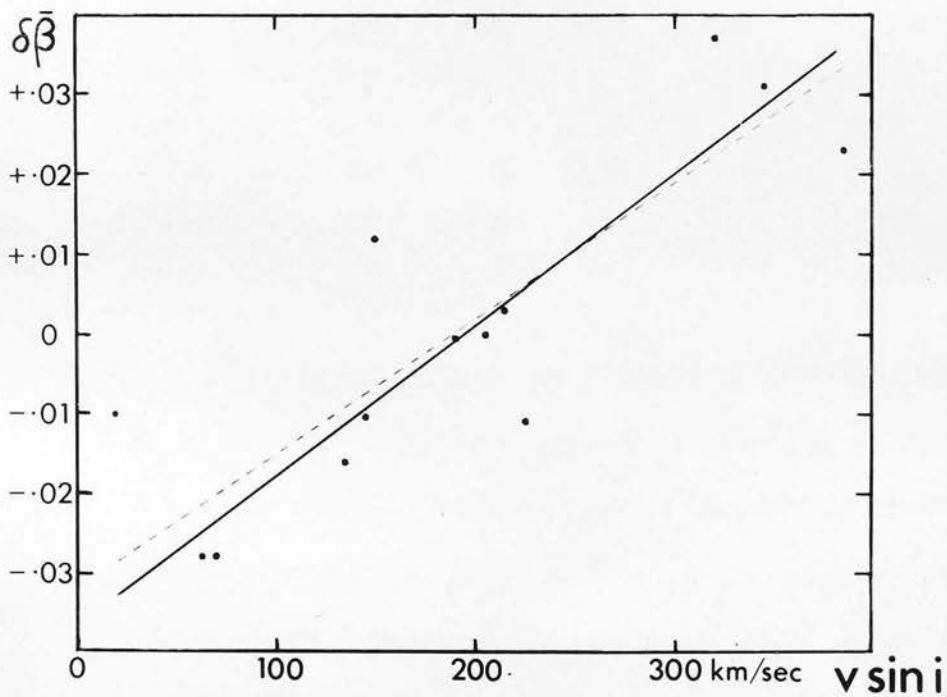


Figure 7  
DEVIATIONS IN  $\bar{\beta}$  FOR THE  
 $\alpha$  PERSEI CLUSTER.

Table 2

 $\alpha$  PERSEI CLUSTER

HD	Mitchell No.	MK	$(U - B)_0$	$\beta$	Transformed $\Gamma$	Transformed $\frac{1}{2}(HY + H\delta)$	$\bar{\beta}$	vsini
20365	383	B3V	-.63	2.688	2.658	2.694	2.680	145
20418	401	B5V	-.54	2.671	2.648	2.672	2.664	320
21071	675	B6V	-.53	2.734	2.739	2.727	2.733	70
21181	735	B9V	-.21	2.787	2.778	2.796	2.787	345
21278	774	B3V	-.60	2.708	2.712	2.705	2.708	63
21362	810	B6V	-.50	2.695	2.687	2.696	2.693	385
21398	831	B9V	-.17	2.849	2.848	2.846	2.848	135
21428	835	B5V	-.60	2.694	2.676	2.672	2.681	190
21455	861	B5V	-.42			2.732	2.732	150
21641	955	B9V	-.29	2.770		2.802	2.786	215
21672	965	B8V	-.35	2.781	2.789	2.768	2.779	225
21931	1082	B9V	-.16			2.835	2.835	205
22136	1153	B8V	-.33			2.785	2.785	25

(iii) Orion association. Various difficulties arise when the above method of analysis is applied to the whole of the Orion association. The Balmer lines of the nebula are in emission (Flather and Osterbrock, 1960), and the reddening law deviates from the  $1/\lambda$  relationship in the region of the nebula (Hallam, 1959). Sharpless (1962) showed that the stars in the "Sword" region centred on the Orion nebula with radius  $1\frac{1}{2}$  degrees are younger than those in the more dispersed "Belt" region, an area of 4 square degrees centred on  $\epsilon$  Orionis. His argument is based on the positions of the stars in each region in the  $HY - (U - B)_0$  diagram,



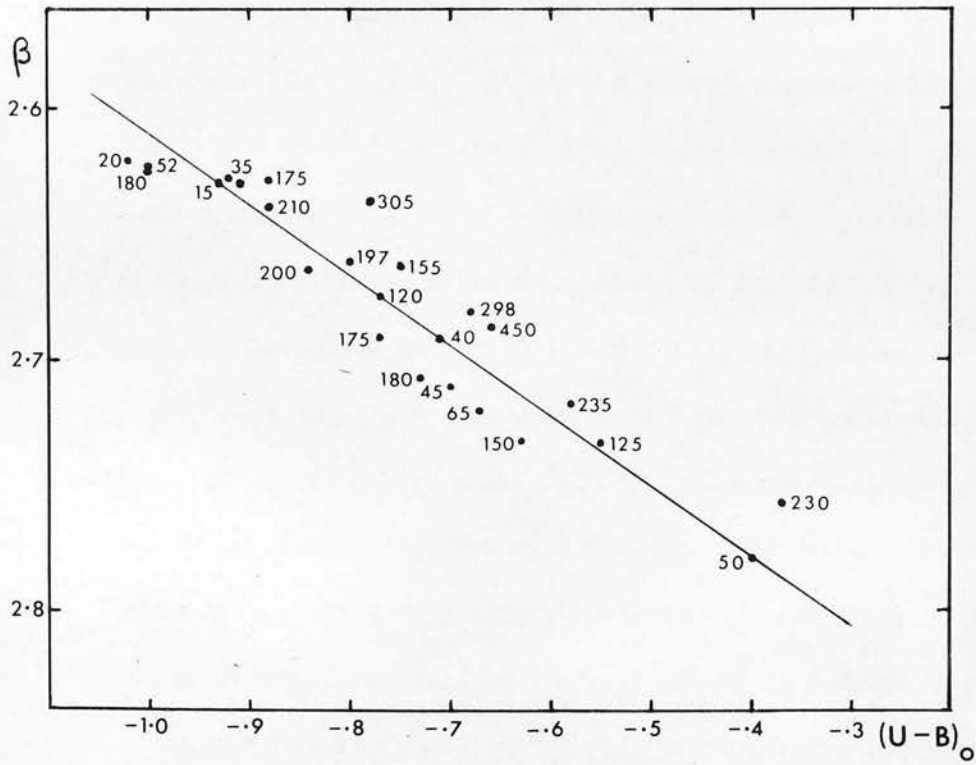


Figure 8

$\beta - (U - B)_0$  DIAGRAM FOR THE ORION ASSOCIATION.

and it would therefore be necessary to check that the mean rotational velocity of the stars in the "Sword" region is not less than that of the stars in the "Belt" region. In view of this probable age difference, the presence of emission lines in the spectrum of the nebula, and the uncertainty of reddening corrections in the region of the nebula, it has been decided to exclude the "Sword" region from discussion.

The UBV photometry by Sharpless (1962) has been used for the stars in the "Belt" region; in other cases the photometry was taken from Sharpless (1952, 1954). Only one  $\Gamma$  observation was taken by Bappu et al. (1962) for most of the stars in the Orion association. An attempt was made to construct a transformation relationship between the  $\beta$  measures by Crawford (1958) and the HY measures by Sharpless (1962), but the standard deviation was  $\pm 0.016$  in  $\beta$ . Only the  $\beta$  measures by Crawford (1958) have therefore been used. The values of  $v_{\text{ sini}}$  are the means of those by Slettebak and Howard (1955), McNamara and Larsson (1962), Abt and Hunter (1962), and McNamara (1963). Only stars classified as luminosity class V from slit spectrograms have been taken. The slope for the deviations, derived from Figs. 8 and 9, is 0.00015 in  $\beta$  per km/sec in  $v_{\text{ sini}}$ . The large scatter in Fig. 9, compared with Figs. 4 and 7 for the Pleiades and  $\alpha$  Persei clusters, may indicate a spread in the ages of the stars in Table 3.

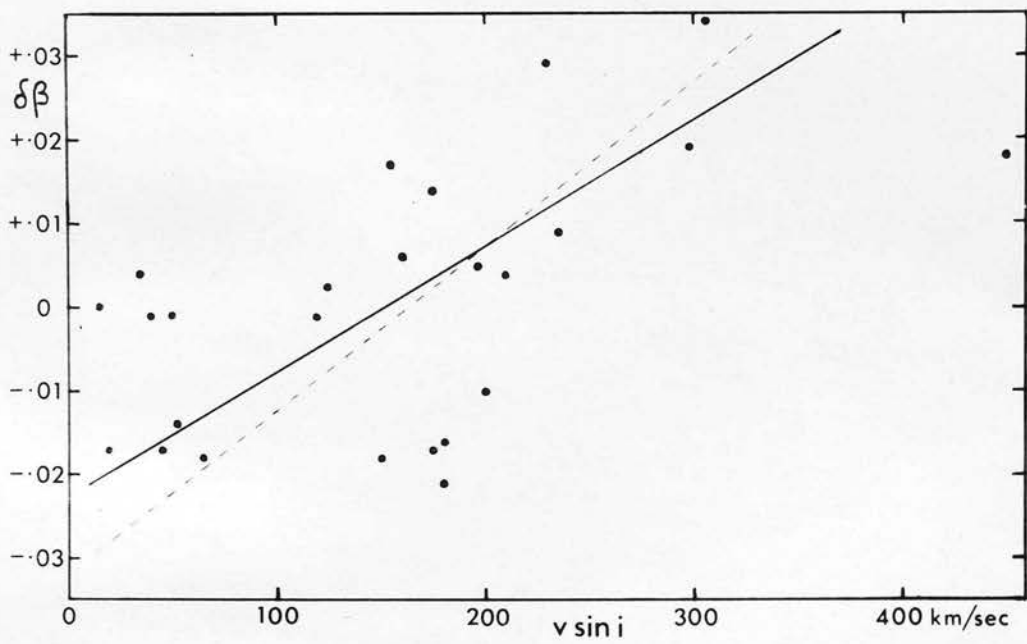


Figure 9

DEVIATIONS IN  $\beta$  FOR THE ORION ASSOCIATION.

Table 3

## ORION ASSOCIATION

HD	BD	MK	$(U - B)_0$	$\beta$	vsini	$\beta +$ 0.00017vsini	$(Q - P)_0$
33647	0°974	B8V	-.40	2.779	50	2.788	0.222
34989	8 933	B1V	-1.00	2.624	52	2.633	0.020
35007	-0 929	B3V	-.71	2.692	40	2.699	0.104
35079	-3 1075	B3V	-.63	2.732	150	2.757	0.119
35299	-0 936	B1V	-.93	2.630	15	2.633	0.040
35407	2 947	B5V	-.66	2.687	450	2.763	0.115
35575	-1 889	B3V	-.77	2.675	120	2.695	0.085
35762	3 903	B2V	-.75	2.663	155	2.689	0.079
35777	-2 1250	B2V	-.78	2.637	305	2.689	0.080
35792	-1 897	B3V	-.67	2.720	65	2.731	0.109
36013	1 1026	B1.5V	-.68	2.681	298	2.732	0.130
36166	1 1032	B1.5V	-.88	2.629	175	2.659	0.056
36392	1 1045	B3V	-.70	2.711	45	2.719	0.110
36591	-1 935	B1V	-1.02	2.621	20	2.624	0.017
36627	3 958	B6V	-.58	2.718	235	2.758	0.152
36695	-1 943	B1V	-1.00	2.626	180	2.657	0.024
36741	1 1058	B2V	-.80	2.661	197	2.695	0.075
36779	-1 949	B3V	-.84	2.664	200	2.698	0.060
36824	5 958	B3V	-.77	2.691	175	2.721	0.082
36954	-0 1009	B3V	-.73	2.707	180	2.738	0.094
37606	1 1088	B8V	-.37	2.757	230	2.796	
37744	-4 1212	B1V	-.92	2.628	35	2.634	
37903	-2 1345	B1.5V	-.88	2.639	210	2.675	
38755	-6 1313	B6V	-.55	2.733	125	2.754	
39291	-7 1187	B2V	-.91	2.629	160	2.656	

There are not sufficient observations to determine the exact relationship between the deviations and  $v_{\text{ sini}}$ . For the above three clusters the relationship has been taken to be linear, and the mean slope is 0.00017 in  $\beta$  per km/sec in  $v_{\text{ sini}}$ . There does not appear to be any large variation of the slope of the deviations with spectral type. However, Sinnerstad (1961) showed that for late A-type and early F-type stars there is no difference in Balmer line intensities for luminosity classes III and V. Since the difference in effective surface gravity between classes III and V is greater for these types than for B-type stars, it is clear that Balmer line intensities are independent of effective surface gravity and therefore of rotation for these later types. Preliminary confirmation of this has been obtained by plotting the photographic measures of  $\frac{1}{2}(H\gamma + H\delta)$  by Ljunggren and Oja (1961) against  $(B - V)_0$  for the Praesepe cluster, and labelling the points with the measures of  $v_{\text{ sini}}$  by Treanor (1960).

Dotted lines of slope 0.00017 in  $\delta\bar{\beta}$  per km/sec in  $v_{\text{ sini}}$  have been fitted to the points in Figs. 4, 7, and 9. The standard deviations from these lines are  $\pm 24$  km/sec for the Pleiades,  $\pm 63$  km/sec for the  $\alpha$  Persei cluster, and  $\pm 86$  km/sec for the Orion association. The approximate mean error in  $\bar{\beta}$  is  $\pm 0.006$  corresponding to  $\pm 35$  km/sec in  $v_{\text{ sini}}$ . The approximate mean error in  $(U - B)_0$  is  $\pm 0.015$  corresponding to  $\pm 0.005$  units of  $\bar{\beta}$  and hence to  $\pm 29$  km/sec in  $v_{\text{ sini}}$ . The approximate mean error in  $v_{\text{ sini}}$  is  $\pm 20$  km/sec. Thus the total observational error is about  $\pm 50$  km/sec. There will also be a contribution to the standard deviations

in Figs. 4, 7, and 9 if there is any non-linearity in the relation between the deviations and  $v \sin i$ . The standard deviations for the Pleiades and the  $\alpha$  Persei clusters are therefore accounted for, but in the Orion association there seems to be an extra source of scatter. The most likely explanation is that there is a spread in the ages of the stars in Table 3.

The above analysis shows that it would be possible to obtain approximate rotational velocities from UBV photometry and  $\beta$  measures for cluster members. This method would be considerably more rapid than the more usual line profile method, for which wide spectra of high dispersion are required. The accuracy obtained would be sufficient for statistical studies of the rotational velocities in clusters. The zero point of the  $v \sin i$  scale for the cluster could be fixed either by measuring the rotational velocities of a few stars from line profiles, or by using the age of the cluster determined from the colour-magnitude diagram. It should be emphasised that the method could be applied only to clusters, and not to associations in which there is likely to be a relatively large spread in the ages of members.

#### Theoretical analysis of the effect of rotation

Sweet and Roy (1953) computed the first-order structure for a rotating Cowling model. They give the following equation for the effect of rotation on the effective surface gravity  $g_s^{\text{eff}}$ .



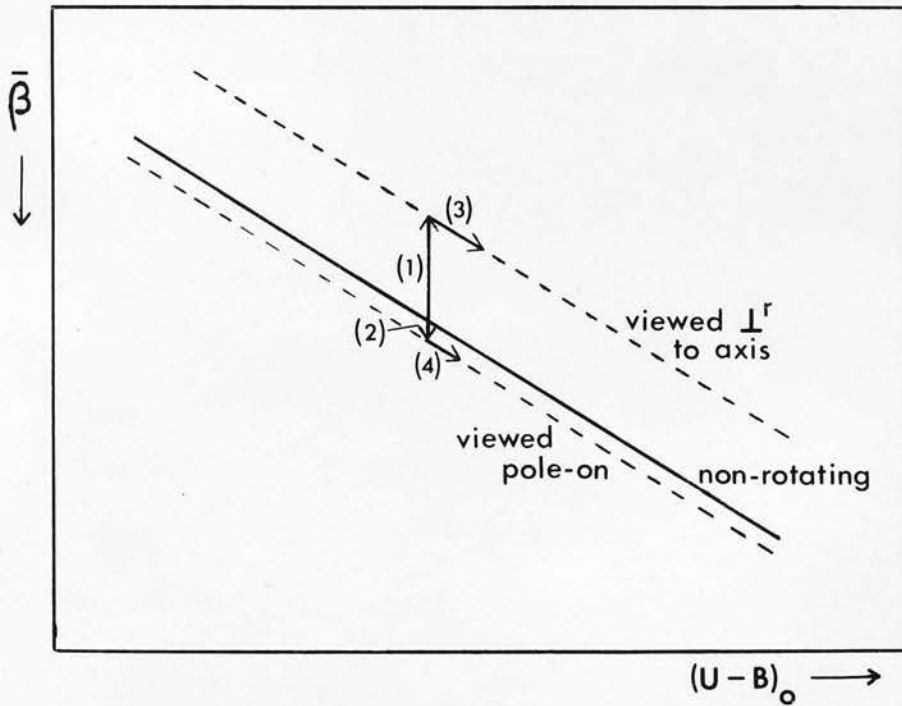


Figure 10  
THE EFFECT OF ROTATION ON THE POSITION OF A  
STAR IN THE  $\bar{\beta} - (U - B)_0$  DIAGRAM.

$$g_s^{\text{eff}} = g_s^{\text{eff}}(0) \left[ 1 - 1.200 \alpha_1 + 1.420 \alpha_1 P_2 \right], \quad (3)$$

where

$$\alpha_1 = \frac{v_0^2}{R g_s(0)} \left[ 1 + 0.772 \frac{v_0^2}{R g_s(0)} \right]. \quad (4)$$

$v_0$  is the equatorial rotational velocity, and  $R$  and  $g_s(0)$  are the radius and surface gravity of a non-rotating star of the same mass. The

Legendre coefficient  $P_2$  is given by

$$P_2 = \frac{1}{2}(3\cos^2\theta - 1), \quad (5)$$

where  $\theta$  is the angular distance from the axis of rotation. When the star is viewed perpendicular to the axis of rotation,  $P_2 = -\frac{1}{2}$ , and

$$g_s^{\text{eff}} = g_s^{\text{eff}}(0) \left[ 1 - 1.91 \alpha_1 \right]. \quad (6)$$

When the star is viewed pole-on,  $P_2 = 1$ , and

$$g_s^{\text{eff}} = g_s^{\text{eff}}(0) \left[ 1 + 0.22 \alpha_1 \right]. \quad (7)$$

Thus the effect of rotation on the effective surface gravity is much smaller when the star is viewed pole-on, and the change in  $\bar{\beta}$  is much less in this case. The changes in  $\bar{\beta}$  for the two cases are indicated by arrows (1) and (2) in Fig. 10. The effective surface temperature  $T_e$  is reduced in both cases; this will increase  $(U - B)_0$  and increase  $\bar{\beta}$ , so that the star is displaced approximately parallel to the main sequence of non-rotating stars of the same age (indicated by arrows (3) and (4) in Fig. 10). The pole-on stars therefore lie only slightly below the non-rotators,

but the effect on stars viewed perpendicular to their axes of rotation is large enough to be observed.

A star of MK type B5V is now considered. From Table 6 of a paper by Pilowski (1950) the radius  $R$  is  $2.20 \times 10^6$  km. The effective surface gravity is given on page 189 of "Astrophysical Quantities" by Allen (1955) as  $0.10 \text{ km/sec}^2$ . The changes  $\delta\bar{\beta}$  in  $\bar{\beta}$  may be calculated from the changes  $\delta \log g_s^{\text{eff}}$  in  $\log g_s^{\text{eff}}$  using the approximate analysis of Sinnerstad (1961) based on the theory by Unsöld (1955). The mean equivalent width of H $\gamma$  and H $\delta$  is given by

$$W_\lambda = 7.12 \times 10^{-6} R_c^{3/5} \left( \frac{N_{O2} H.P_e}{T} \right)^{2/5} \quad (8)$$

Sinnerstad computed the number of hydrogen atoms capable of absorbing the Balmer lines  $N_{O2}$ , the electron pressure  $P_e$ , and the temperature  $T$  from the models for the stellar atmosphere constructed by Vitense (1951). He calculated the central depth of the lines  $R_c$  using the Kirchhoff-Planck function, and constructed a diagram for H $\gamma$  and H $\delta$  giving  $W_\lambda$  and  $R_c$  in terms of  $\theta_e = 5040/T_e$  and  $\log g_s^{\text{eff}}$ . Since  $\bar{\beta}$  has been determined mainly H $\beta$  and H $\gamma$  instead of H $\gamma$  and H $\delta$ , a small error will be introduced by using this diagram. The changes  $\delta W_\lambda$  in  $W_\lambda$  have been converted to changes  $\delta\bar{\beta}$  in  $\bar{\beta}$  using the relation given by Crawford (1958) between  $\beta$  and the equivalent widths  $W$  of H $\gamma$  measured by Petrie.

$$W = -16.7 + 34(\beta - 2.000) \quad (9)$$

In Table 4 the changes of  $\delta\bar{\beta}$  due to rotation have been calculated for

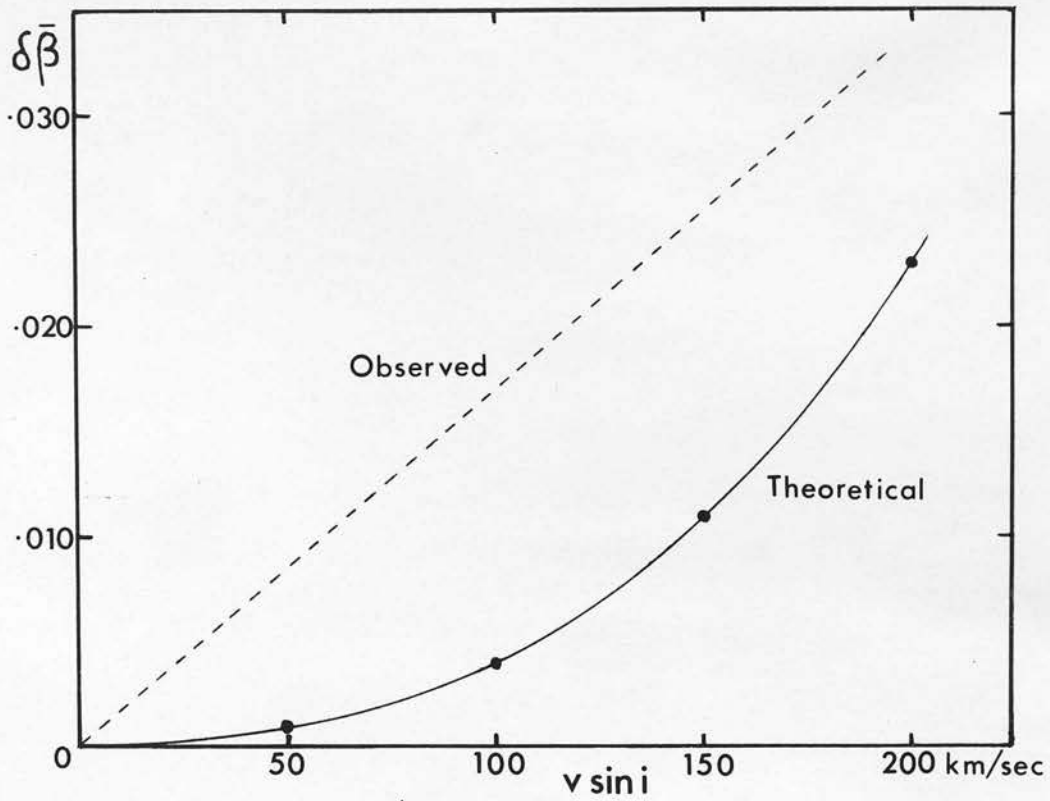


Figure 11

COMPARISON OF THEORETICAL AND OBSERVED DEVIATIONS IN  $\bar{\beta}$ .

various values of  $v_o$  for stars viewed perpendicular to the axis of rotation and pole-on. It will be seen that these changes are small in the pole-on case. In the case of stars viewed perpendicular to their axes of rotation,  $v_o = v \sin i$ , and the changes have been compared in Fig. 11 to the observed slope of 0.00017 in  $\bar{\beta}$  per km/sec in  $v \sin i$ . In using Sinnerstad's diagram to find  $\delta W_\lambda$  from  $\delta \log g_s^{\text{eff}}$  the mean values of  $W_\lambda$  and  $R_c$  for B5V stars have been taken as 6.8 and 51 respectively from his spectrophotometry.

Table 4

$v_o$ in km/sec	Viewed perpendicular to axis of rotation					Viewed pole-on		
	$\alpha_1$	$g_s^{\text{eff}}$	$\delta \log g_s^{\text{eff}}$	$\delta \bar{\beta}$	Observed $\delta \bar{\beta}$	$g_s^{\text{eff}}$	$\delta \log g_s^{\text{eff}}$	$\delta \bar{\beta}$
0	0.0000	$1.000 g_s^{\text{eff}}(0)$	0.000	0.000	0.000	$1.000 g_s^{\text{eff}}(0)$	0.000	0.000
50	0.0115	$0.978 g_s^{\text{eff}}(0)$	0.010	0.001	0.0085	$1.003 g_s^{\text{eff}}(0)$	0.001	0.000
100	0.0470	$0.910 g_s^{\text{eff}}(0)$	0.041	0.004	0.017	$1.010 g_s^{\text{eff}}(0)$	0.004	0.000
150	0.1103	$0.789 g_s^{\text{eff}}(0)$	0.103	0.011	0.0255	$1.024 g_s^{\text{eff}}(0)$	0.010	0.001
200	0.2072	$0.604 g_s^{\text{eff}}(0)$	0.219	0.023	0.034	$1.046 g_s^{\text{eff}}(0)$	0.019	0.002

The model used by Sweet and Roy breaks down formally when  $\alpha_1$  is greater than 0.22 since the surface density at the equator then becomes negative, and a second order model is required for rapidly rotating stars. The above analysis shows that the surface gravity explanation gives the correct order of magnitude for the observed effect of rotation. Exact agreement between the theoretical and observed results is not to

be expected in view of the various approximations in the theory. For example, Unsöld's analysis is based on the Holtsmark theory of Stark broadening which considers only the ions and neglects the contribution to broadening by the electrons.

## CHAPTER 3

### SPECTRAL CLASSIFICATION AT LOW DISPERSION

#### Introduction

The MK system of spectral classification defined by Johnson and Morgan (1953) is the one in general use. It depends on visual inspection of lines in the blue region of the spectrum and gives a two-dimensional classification in terms of spectral type and luminosity class. A dispersion of about 120 Å/mm is normally required. The most successful attempt at determining MK types of early-type stars at a lower dispersion (225 Å/mm at HY) was that by Chalonge and Divan (1952) using spectrophotometric measurements of the size D and the position  $\lambda_1$  of the Balmer discontinuity. This method has the advantage of being less sensitive to variations in chemical abundance from star to star, since it depends on hydrogen which is the most abundant element.

#### Classification on objective prism spectra

An investigation has been carried out on objective prism plates taken with the Edinburgh 16/24-inch Schmidt telescope at a dispersion of 1000 Å/mm at HY to decide whether classification of B-type stars using quantities similar to  $\lambda_1$  and D is possible. This low dispersion would allow large numbers of faint stars to be classified.

The Ilford SRO emulsion, which is sensitive in the ultraviolet and



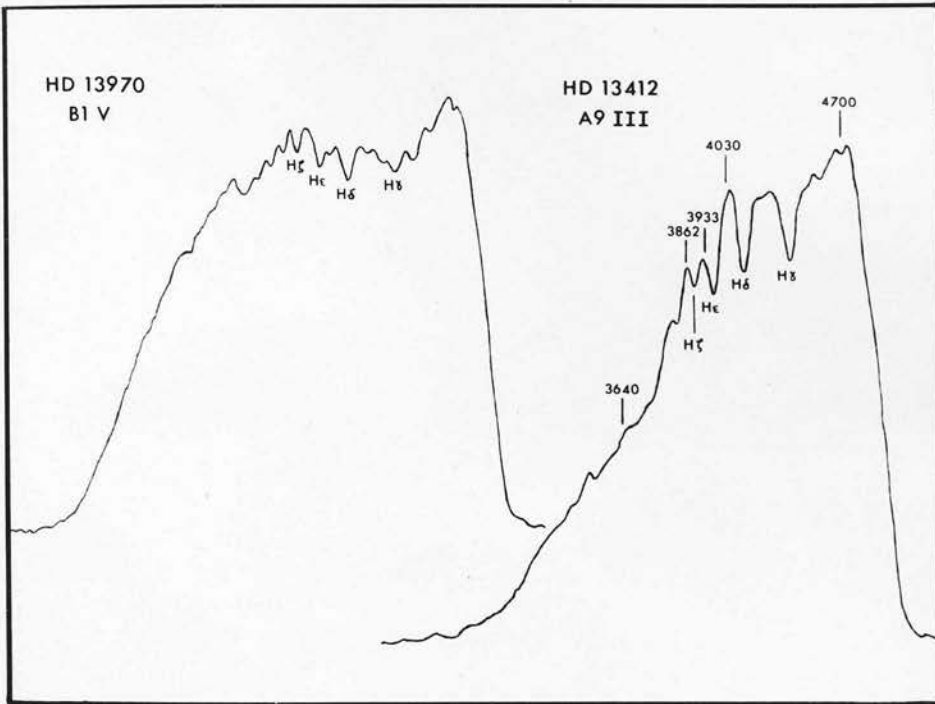


Figure 1

MICRODENSITOMETER TRACINGS.

the blue as far as 4900A, has been used. However, owing to the increase in dispersion and atmospheric absorption towards the ultraviolet, stars correctly exposed in the blue region are badly underexposed in the ultraviolet region. A Kodak CC50Y gelatine filter has therefore been inserted to absorb part of the blue light, so that measurements may be made on the Balmer discontinuity. The spectra are widened (usually to 0.3 mm) by varying the sidereal drive rate. Each plate covers a circular region 3.8 degrees in diameter.

The spectra are traced on a Joyce-Loebl microdensitometer with a projected slit width of 50  $\mu$  and a tracing to plate magnification of 50. Typical tracings of early-type stars are shown in Figs. 1 and 2. The Baker density

$$\Delta = \log_{10} \frac{1 - T}{T},$$

where T is the transmission, has been used in the analysis of the plates, since its relation to magnitude is approximately linear (Baker, 1949). This eliminates the determination of the characteristic curve for each plate.

Since the Balmer discontinuity has a maximum value at spectral type A1 for main sequence stars, it is first necessary to separate stars earlier and later than A1. The intensity of the CaII K-line at 3933A increases towards later spectral types, but the line does not normally

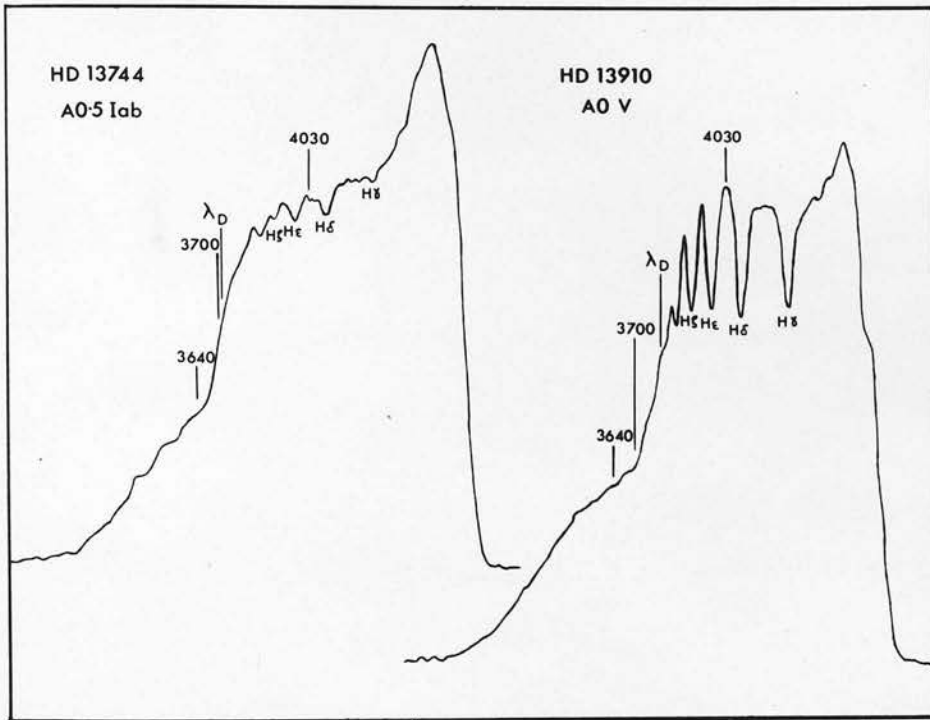


Figure 2

MICRODENSITOMETER TRACINGS.

become visible on the tracings until the F-type stars. However, its effect may be measured in the A-type stars from the depression which it causes in the continuum between H $\epsilon$  and H $\zeta$ . The quantity

$$K = \frac{1}{2}(\Delta_{3862} + \Delta_{4030}) - \Delta_{3933}$$

may therefore be taken as a measure of the intensity of the CaII K-line.

The quantity

$$C_D = (\Delta_{4030} - \Delta_{3640}) - 0.75(\Delta_{4700} - \Delta_{4030})$$

is related to the size of the Balmer discontinuity and is independent of interstellar reddening if the  $1/\lambda$  law holds. The wavelength  $\lambda_D$  of the Balmer discontinuity is defined as the wavelength at which

$$\Delta = \frac{1}{2}(\Delta_{3640} + \Delta_{4030}).$$

Supergiants are recognised by their small values of  $\lambda_D$ . For the other early-type stars on the plate,  $C_D$  is plotted against  $K$ , and stars earlier and later than A1 are separated by their positions in this diagram. No confusion between B and A-type stars arises in the case of supergiants, since  $C_D$  increases until spectral type A9.

As an example, the analysis of a Schmidt plate is given in Table 1 for a region in Cygnus (centred at  $\alpha_{1950} = 20^h 12^m$ ,  $\delta_{1950} = +37^\circ 22'$ ) for which Barbier (1962) has determined MK types from objective prism spectra at a dispersion of about 80 A/mm at HY.  $K$  and  $C_D$  are listed for all measurable stars in the spectral type range B3 to F5. Fig. 3 shows

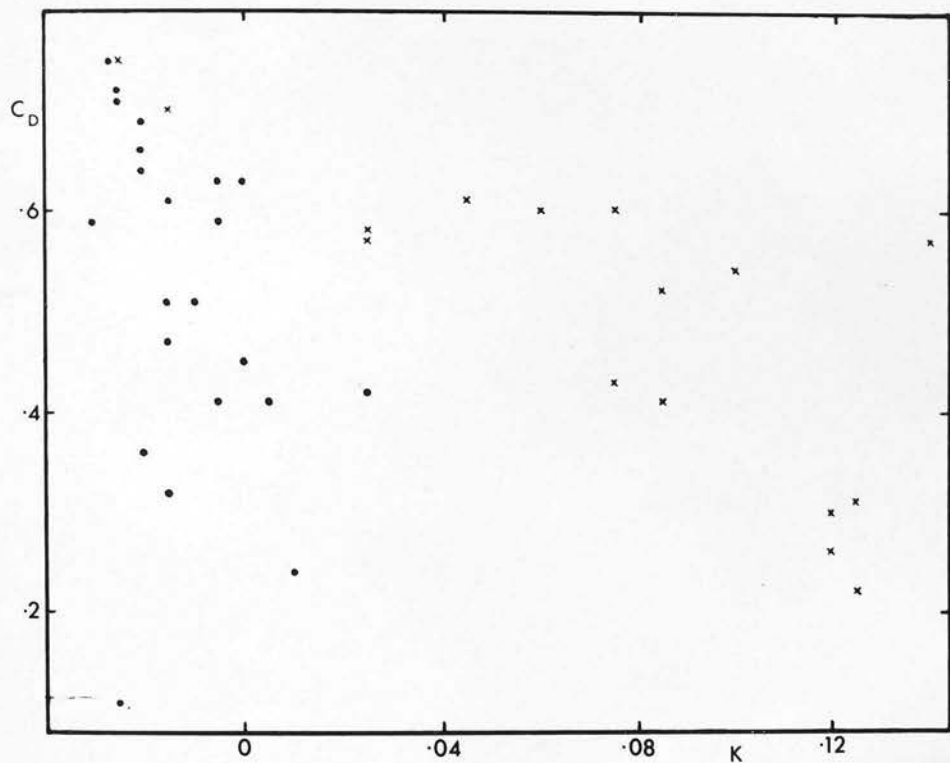


Figure 3

SEPARATION OF STARS EARLIER AND LATER THAN A1. FILLED CIRCLES DENOTE STARS OF TYPE A0 AND EARLIER; OTHER STARS ARE SHOWN BY CROSSES.

Table 1

## MEASURES FOR THE CYGNUS REGION

HD	BD	Barbier MK	Edinburgh K	Uppsala K	C <sub>D</sub>
190700	37 <sup>0</sup> 3754	A0IV	-.025	20	.72
191025	36 3873	A1V	.025	45	.58
191024	38 3905	B8II	-.015	14	.51
191176	37 3772	A1III	-.025	25	.75
191225	37 3774	A0V	-.025	23	.71
191257	38 3913	A3IV	.045	43	.61
191378	36 3891	B9.5V	.005	28	.41
191472	37 3787	A5Ib	.06	41	.65
191494	35 3988	B3V	-.015	18	.61
191720	36 3916	B9V	-.01	17	
228079	36 3918	B8II	.00	27	.45
228163	37 3808	A0IV	-.02	21	.64
228171	37 3809	B9V	-.015	18	.32
192102	38 3941	B8IV	-.03	15	.59
192123	38 3942	B8IV	-.005	33	.41
192283	36 3933	B9.5V	-.005	20	.63
	37 3827	F0III	.235	79	.35
192361	38 3952	B8III	.025	25	.42
192382	36 3937	A1:V	.00	33	.56
228403	36 3941	A7III	.12	45	.26
228426	36 3943	A7III	.085	53	.41
192537	37 3834	B3V	-.005	19	.59
228475	37 3839	A2IV	.06	48	.60
228485	36 3952	A5III	.075	62	.43

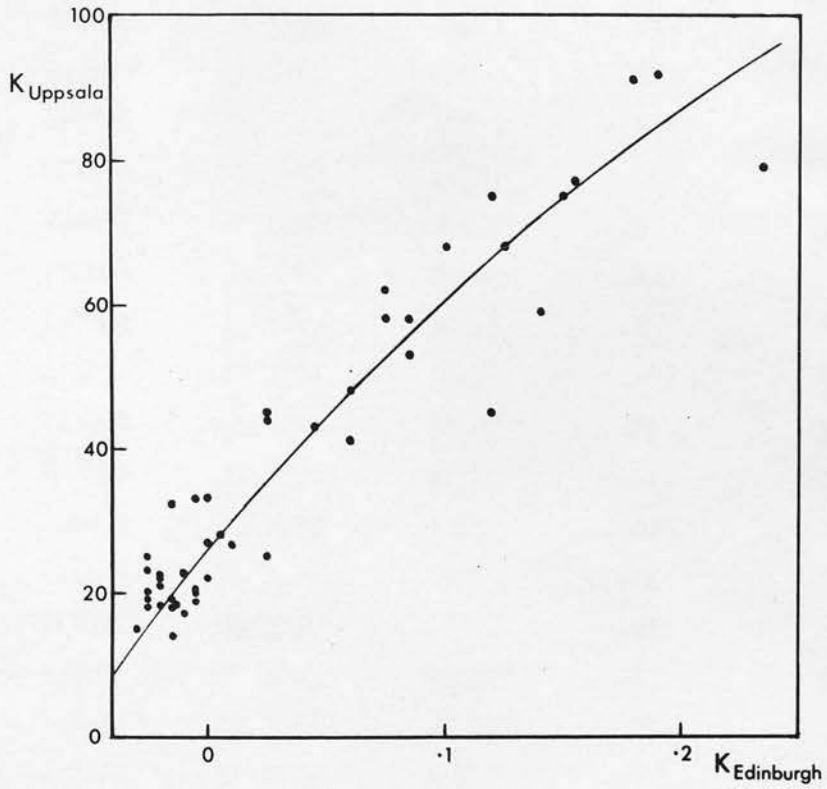


Figure 4

COMPARISON BETWEEN MEASURES OF THE CaII K-LINE  
AT UPPSALA AND EDINBURGH.



Table 1 (continued)

## MEASURES FOR THE CYGNUS REGION

HD	BD	Barbier MK	Edinburgh K	Uppsala K	$C_D$
192604	35 <sup>0</sup> 4031	B7III	-.01	23	.51
228486	36 3954	B8III	-.015	19	.47
228509	37 3842	A3V	.075	58	.60
192745	36 3962	A0V	-.025	19	.75
228598	37 3852	A3IV	-.015	33	.70
228657	37 3855	B8V	-.02	23	.66
192988	36 3980	F0IV	.125		.22
193033	37 3863	A9III	.15	75	
193184	37 3868	F2II	.155	77	.20
193204	35 4054	F2III	.18	91	.10
228791	38 3991	B4IV	.01	27	.24
228807	37 3873	B3IV	-.025	18	.11
193268	36 3994	F5IV	.19	92	.12
193290	36 3996		-.005	20:	.63
193537	37 3883	B9.5IV	-.02	22	.69
193612	37 3889	A0III	-.02	18	.36
193635	36 4009	A3V	.025	44	.57
193636	35 4069	A7V	.14	59	.57
229020	36 4019	A7IV	.10	68	.56
229041	38 4030	A9III	.125	68	.31
193815	36 4020	A9III	.12	75	.30
193927	36 4027	A5III	.085	58	.52
193984	37 3904	A0V	.00	22	.63

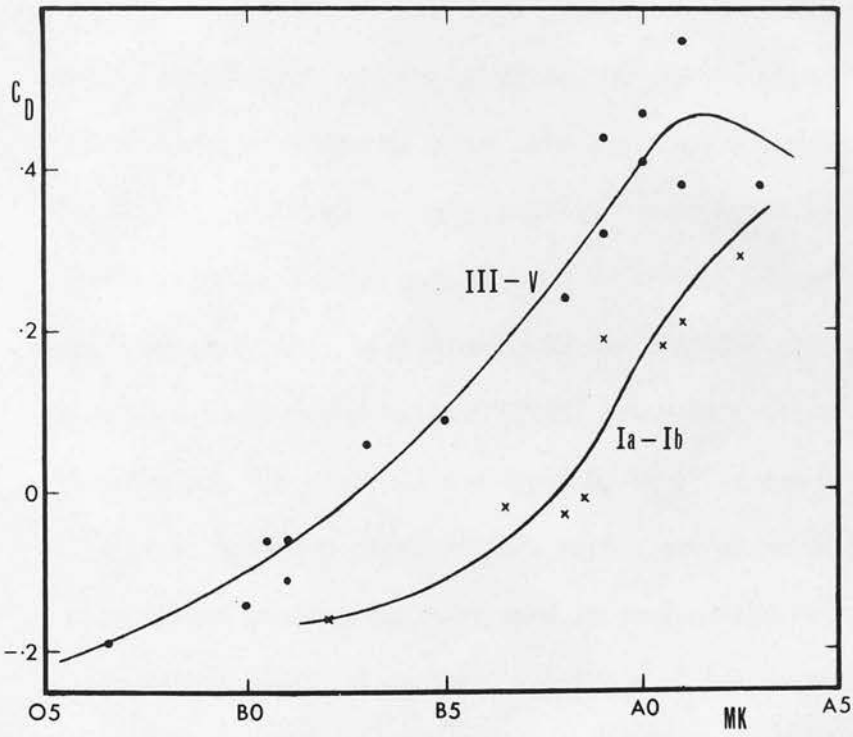


Figure 5

CLASSIFICATION BY  $C_D$ .

the separation of stars earlier and later than A1 from the plot of  $C_D$  against K. The relation between K and measures of the intensity of the CaII K-line by Malmquist, Ljunggren and Oja (1960) at Uppsala Observatory on objective prism plates at a dispersion of about 300 Å/mm at HY is shown in Fig. 4.

A suitable region for investigating the possibility of classifying B-type stars from measures of  $C_D$  and  $\lambda_D$  is the region of the h and  $\chi$  Persei cluster, since MK types have been determined from slit spectra for both supergiants and main sequence stars by Bidelman (1943) and Hiltner (1956). Luminosity classes have been deduced from Bidelman's absolute magnitudes by referring to the absolute magnitude calibration by Morgan, Keenan and Kellman (1943) which he employed. The adopted MK types are the means of the types by Bidelman and Hiltner. Measures of  $C_D$  and  $\lambda_D$  for a plate of this region are given in Table 2. A coarse nylon thread grating has been used in conjunction with the prism so that stars with a range of apparent magnitude of two magnitudes may be measured from the centre or first order images.  $C_D$  has been plotted against the adopted MK types in Fig. 5. Classification from  $C_D$  to an accuracy of one subclass in spectral type results, provided that supergiants are first separated from the other stars. A calibration for each plate is, however, required, since  $C_D$  depends on the atmospheric transparency and the slope of the characteristic curve for the plate. An approximate

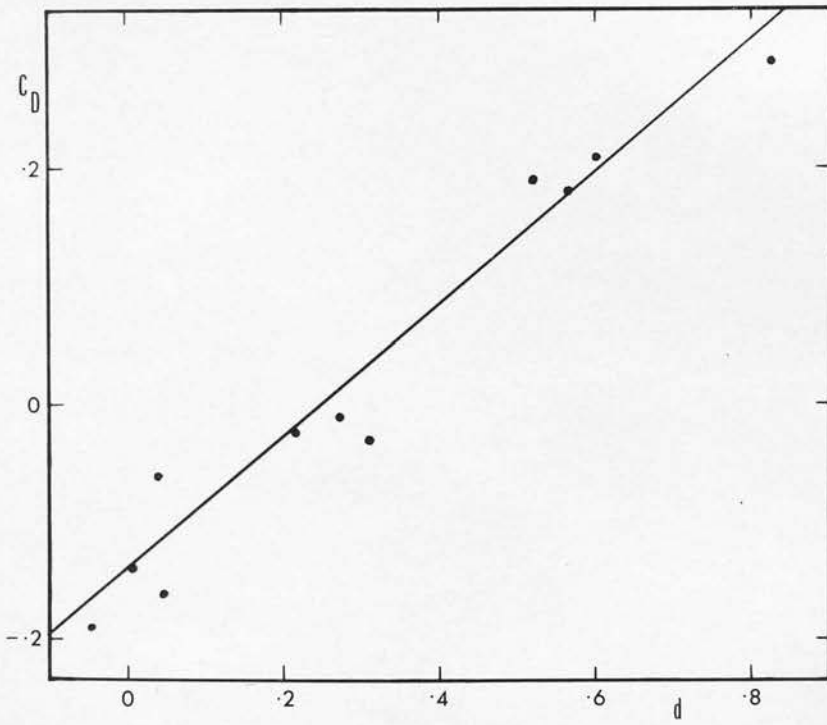


Figure 6

Table 2

MEASURES FOR THE  $\eta$  AND  $\chi$  PERSEI CLUSTER REGION

HD	Hiltner MK	Bidelman MKK	Adopted MK	$C_D$	d	$\lambda_D - 3700$
12994		B8IV-V	B8IV-V	.24		96
13267	B5Ia	B8Ia	B6.5Ia	-.02	.216	18
13476	A3Iab	A2Iab	A2.5Iab	.29	.827	24
13716	B0.5III	B0.5II	B0.5II-III	-.06	.039	
13744	A0Iab	A1Iab	A0.5Iab	.18	.566	23
13910		A0Vn	A0V	.47		89
13970		B1Vn	B1V	-.11		
14210		B9IV	B9IV	.44		63
14322	B8Ib	B8Ia	B8Iab	-.03	.311	15
14331	B0III	B0II	B0II-III	-.14	.004	
14433	A1Ia	A1Ia	A1Ia	.21	.601	14
14434	O6	O7n	O6.5	-.19	-.049	
14542	B8Ia	B9Ia	B8.5Ia	-.01	.270	16
14581		B9III	B9III	.32		37
14646		A0V	A0V	.41		58
14818	B2Ia	B2Ia	B2Ia	-.16	.045	
14825		A3V	A3V	.38		
14871		B5V	B5V	.09		73
14899	B8Ib	A0Iab	B9Ib	.19	.521	15
15124		B3:V	B3:V	.06		101
15240		A1V	A1V	.56		69
15324	BLIV		BLIV	-.06		
15332		A1V	A1V	.38		104

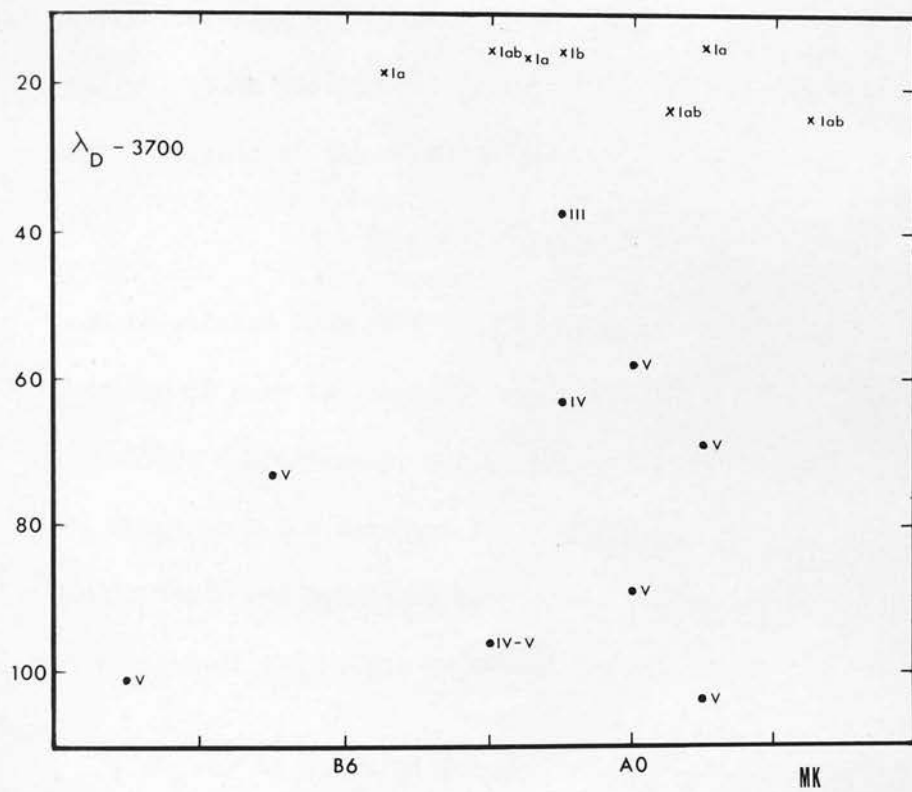


Figure 7

LUMINOSITY CLASSIFICATION FROM MEASURES OF  $\lambda_D$ .

calibration may be obtained by using values of  $(U - B)_0$  from MK types or UBV photometry in the literature, or from the fact that on a plate with a large number of stars the range in  $C_D$  corresponds to a range in spectral type from 0 to A1. A more satisfactory method of calibration is by measuring the Balmer discontinuity for some stars by narrow-band photoelectric photometry. A calibration of this type is shown in Fig. 6 for the plate of the  $\eta$  and  $\chi$  Persei cluster region. The quantity

$$d = (Q - N) - 1.3(N - M)$$

was calculated from photoelectric measures by Borgman (1960). The wavelengths of peak transmission of the Q, N and M filters are 3560, 4055 and 4550A respectively, and these wavelengths correspond fairly closely to those used for defining  $C_D$ . The half-width of the Q filter is 90A, while the N and M filters both have half-widths of 200A. The standard deviation of the points in the calibration is  $\pm 0.06^m$ .

$\lambda_D$  may be measured for stars later than spectral type B2. The values of  $\lambda_D - 3700$  for the  $\eta$  and  $\chi$  Persei cluster region are plotted in Fig. 7 to show that  $\lambda_D$  may be used for luminosity classification. From a comparison between the values of  $\lambda_D$  on two different plates the mean error in the values of  $\lambda_D$  from one plate is  $\pm 5A$ . No plate calibration for  $\lambda_D$  is required, since measures on several plates showed no systematic variations from plate to plate.



## CHAPTER 4

### MEASUREMENT OF ROTATIONAL VELOCITIES

#### Previous work

The first observation of stellar rotation was by Schlesinger (1909) who noticed the distortions in the radial velocity curve of the eclipsing binary  $\delta$  Librae. Shajn and Struve (1929) measured line widths of spectroscopic binaries and demonstrated the presence of fast rotation in binaries of short period. They also discussed the effect of rotation on line profiles. Elvey (1930) developed a graphical method of measuring rotational velocities. Using the profiles of MgII 4481 for two sharp-line stars, the profiles for stars with various rotational velocities were deduced by dividing the stellar disc into strips parallel to the axis of rotation and summing the contributions of the strips allowing for the Doppler displacement of each strip. Slettebak (1949, 1954) refined the method by applying a correction for limb darkening. Since the angle of inclination  $i$  between the axis of rotation and the line of sight is generally unknown, only the component  $v \sin i$  of the equatorial rotational velocity  $v$  can be determined. For many purposes, therefore, large numbers of stars must be measured so that a statistical analysis may be applied.

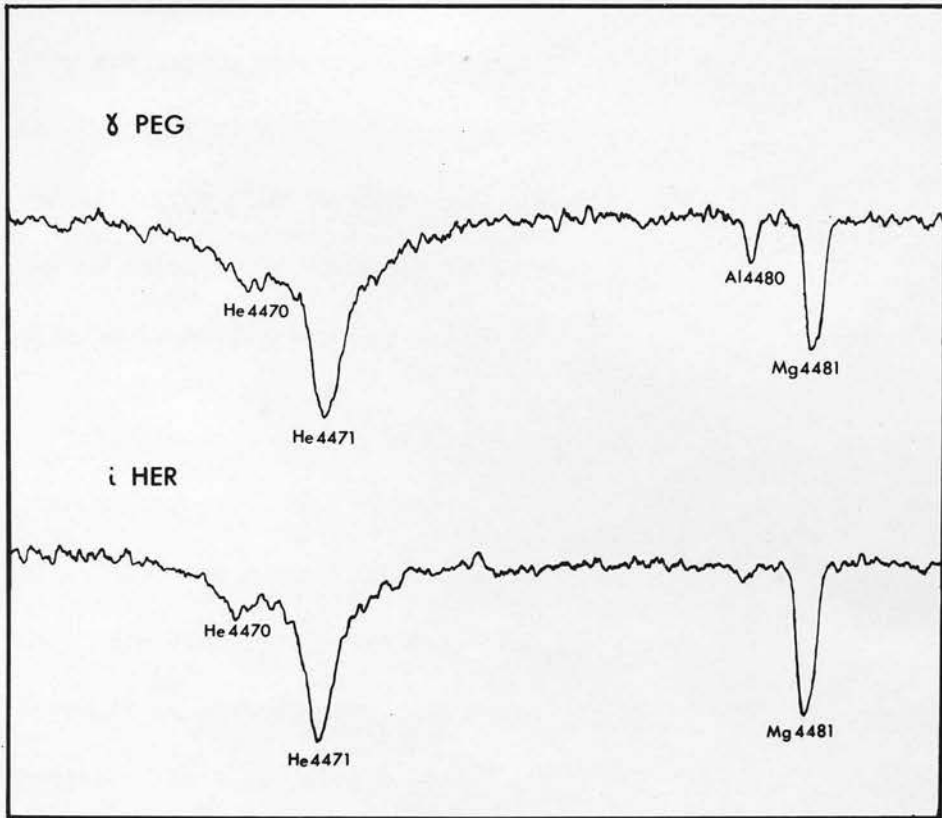


Figure 1  
MICRODENSITOMETER TRACINGS OF THE HeI 4471 AND MgII 4481 LINES  
FOR THE STARS  $\gamma$  PEG AND  $i$  HER.

Various attempts have been made to eliminate the labour of determining a line profile for each star. These have included measurement of line widths by micrometer wire settings and estimates by visual comparison with standards. Both methods are liable to give systematic errors, especially if the spectra are not all of the same density or if there is a large variation of equivalent width of the line from star to star. However, accurate rotational velocities may be obtained by measuring half-widths on a density-recording microphotometer (e.g. Abt and Hunter, 1962).

In the case of B-type stars, the choice of spectral lines presents some difficulty. For the early B stars most of the work on rotational velocities has been based on the HeI 4471 line. Struve (1929) showed that this line is blended with the forbidden line HeI 4470, which is stronger in main sequence stars than in supergiants. From a set of spectra with a dispersion of 4.7 Å/mm taken by Dr. H. E. Butler at the Mount Wilson Observatory, microdensitometer tracings of the HeI 4471 line are shown in Fig. 1 for the stars  $\epsilon$  Her (B3IV) and  $\gamma$  Peg (B2IV) which have zero rotational velocity. In view of this blend with HeI 4470, it is desirable to measure several helium lines, and the most suitable lines in the blue region of the spectrum are HeI 4026, HeI 4144, and HeI 4388. The helium lines are also strongly affected by Stark broadening, the wings of HeI 4471 being clearly visible in Fig. 1. This should be taken into account in any comparison between the mean

rotational velocities of various luminosity classes. The only measurable lines not broadened by the Stark effect are MgII 4481 and CII 4267. The MgII 4481 line is blended with AlIII 4480 for spectral types earlier than B5, and the rather weak CII 4267 line is the best if the dispersion is sufficiently high. For the late B stars, MgII 4481 is the only measurable line; it is unblended but is somewhat weaker than the HeI lines in the early B stars.

#### Measurement of rotational velocities using the Balmer lines

Rotational velocities have been determined for the majority of B-type stars brighter than  $m_v = 5.5$  and for the stars in some of the nearby clusters and associations. Since many interesting problems will require rotational velocities of large numbers of fainter stars, methods of determining  $v \sin i$  from spectra of low dispersion and width would be useful. Examination of the cores of the Balmer lines shows that their profiles depend mainly on  $v \sin i$  and to a lesser extent on Stark broadening. It should therefore be possible to determine rotational velocities from the Balmer lines which are always strong in the B-type stars.

Spectra of 50 stars of types B2 to A1 were taken with the slit spectrograph at the Cassegrain focus of the Edinburgh 36-inch telescope. The grating and f/1 Schmidt camera of the spectrograph gave a dispersion of 60Å/mm, the wavelength range being 3600 to 4550Å.

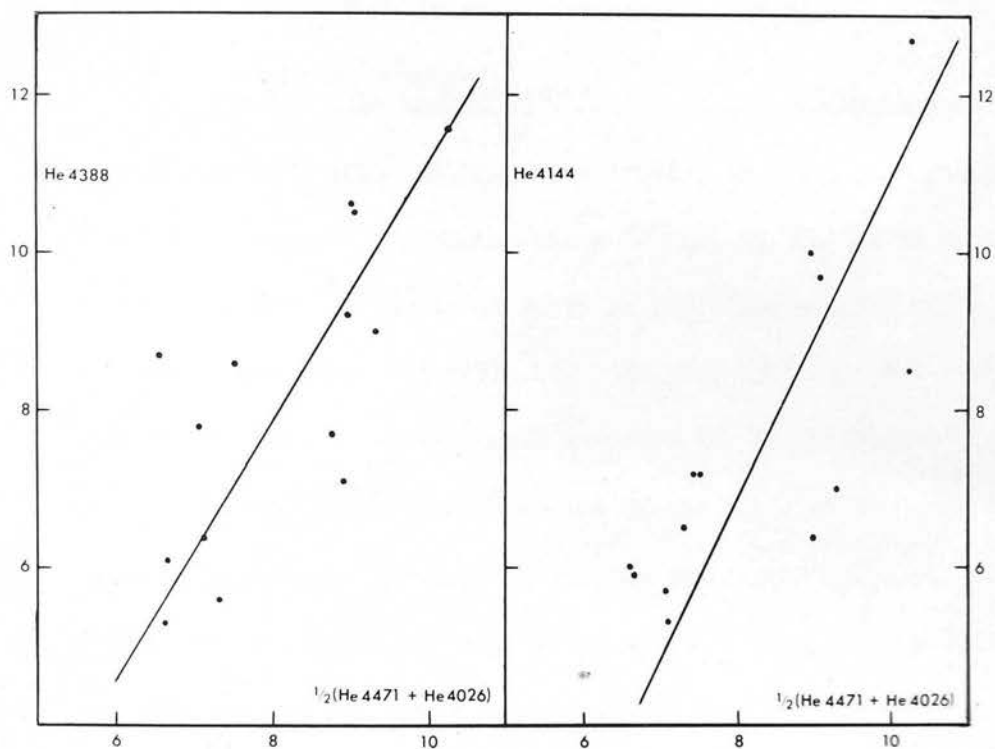


Figure 2

THE WIDTHS OF HeI 4388 AND HeI 4144 PLOTTED AGAINST THE AVERAGE WIDTH OF HeI 4471 AND HeI 4026.

The slit width projected on the plate was  $10\mu$ . Kodak IIaO emulsion was used, and the spectra were widened to 0.3mm by a rocking plate. One good spectrum was obtained for each star. The stars include 32 standards of luminosity classes III to V with measures of vsini by Slettebak (1954) or Slettebak and Howard (1955). Emission line and peculiar stars were excluded.

The spectra were traced on a Joyce-Loebl microdensitometer using a projected slit width of  $50\mu$  and a tracing to plate magnification of 100. The widths of the Balmer lines H $\gamma$ , H $\delta$ , H $\epsilon$ , H $\eta$  and H $\theta$  were measured at 4/10 and 8/10 of the total depth on the Baker density scale and the widths of MgII 4481, HeI 4471, HeI 4388, HeI 4026, and HeI 4144 were measured at half the total depth whenever the strength of the line permitted. The mean widths  $\bar{H}$  of the Balmer lines at 4/10 and 8/10 of the total depth are given in mm. on the tracing in Table 1. The widths of HeI 4388 and HeI 4144 are plotted against the average width of HeI 4471 and HeI 4026 in Fig. 2 to transform the widths of all the HeI lines to the same system. The mean widths  $\overline{\text{HeI}}$  have been calculated by averaging the widths (or the transformed widths in the case of HeI 4388 and HeI 4144) giving equal weight to each of the four HeI lines; they are listed with the number of lines measured in Table 1. The widths of MgII 4481 are also given.

The mean widths  $\bar{H}$  of the Balmer lines at 8/10 of the total depth are plotted for the standard stars against vsini in Fig. 3. Each point

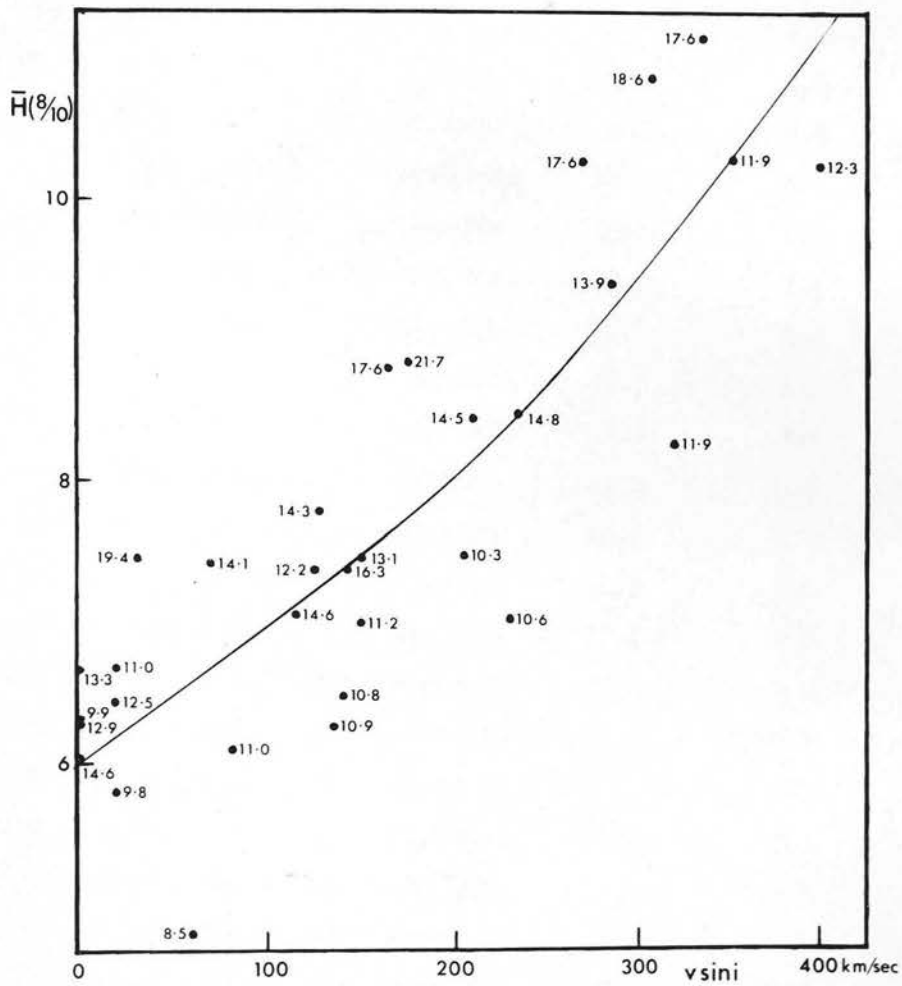


Figure 3

RELATION BETWEEN THE MEAN WIDTHS  $\bar{H}$  OF THE BALMER  
LINES AT 8/10 OF THE TOTAL DEPTH AND  $v \sin i$ .





Table 1

## MEASURES OF LINE WIDTHS

HD	Name	MK	vsini	Group	$\bar{H}$ at 4/10 total depth	$\bar{H}$ at 8/10 total depth	$\bar{H}\epsilon I$	Width of Mg 4481
3360	$\zeta$ Cas	B2V	20	standard	15.6	5.8	7.1	
6300	HR302	B3V		Cas-Tau	18.2	7.1	9.05	
16004	HR746	B3IV		field	18.1	6.0		
20418	31 Per	B5V	320	standard	20.2	8.3	13.0	
21661	HR1059	B3III*		$\alpha$ Persei	14.1	5.2		5.2
27192	HR1333	B2IV		Cas-Tau	15.5	6.9	8.85	
32630	$\eta$ Aur	B3V	125	standard	19.6	7.4	8.5	
34233	HR1719	B3IV		Cas-Tau	20.5	7.0	9.2	6.5
35468	$\gamma$ Ori	B2III	60	standard	13.3	4.8	6.8	
35497	$\beta$ Tau	B7III	82	standard	17.1	6.1		
36881	HR1883	B3III		field	14.8	5.5		5.1
37367	HR1924	B2V		Cas-Tau	13.5	5.6	7.25	
37519	HR1938	B7V		field	21.3	8.8		
39698	HR2052	B2V		Cas-Tau	16.2	6.8	9.3	
42560	$\xi$ Ori	B3V	230	standard	17.6	7.0	9.8	
42818	HR2209	A0V	308	standard	29.5	10.9		
48879	42 Cam	B3IV	140	standard	17.3	6.5	7.7	
49340	43 Cam	B7IV	205	standard	17.8	7.5		
73262	$\delta$ Hya	A0V	270	standard	27.9	10.3	14.3	
74280	$\eta$ Hya	B3V	135	standard	17.2	6.3	8.85	
75137	$\rho$ Hya	A0V	142	standard	23.7	7.4		7.8
87887	$\alpha$ Sex	A0III	0	standard	20.0	6.7		5.0
87901	$\alpha$ Leo	B7V	352	standard	22.2	10.3		
90994	30 Sex	B6V	115	standard	21.7	7.1	8.15	6.1
91130	33 LMi	A0IV		field	24.6	7.8		

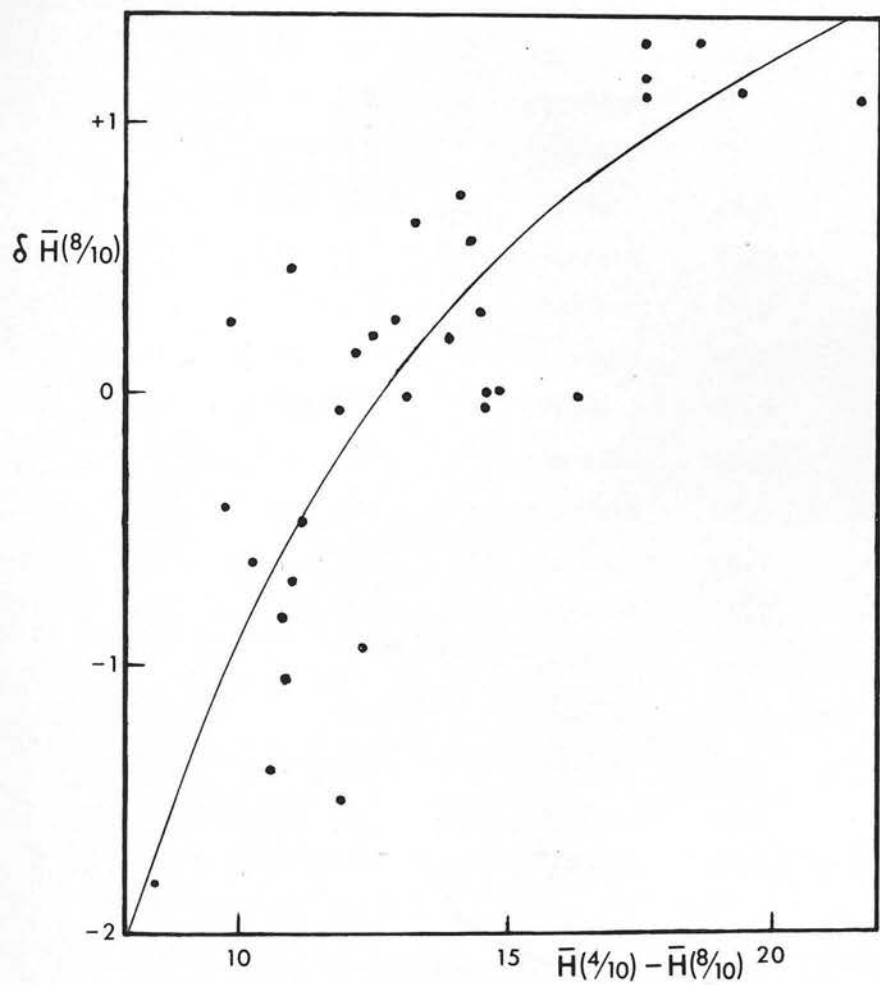
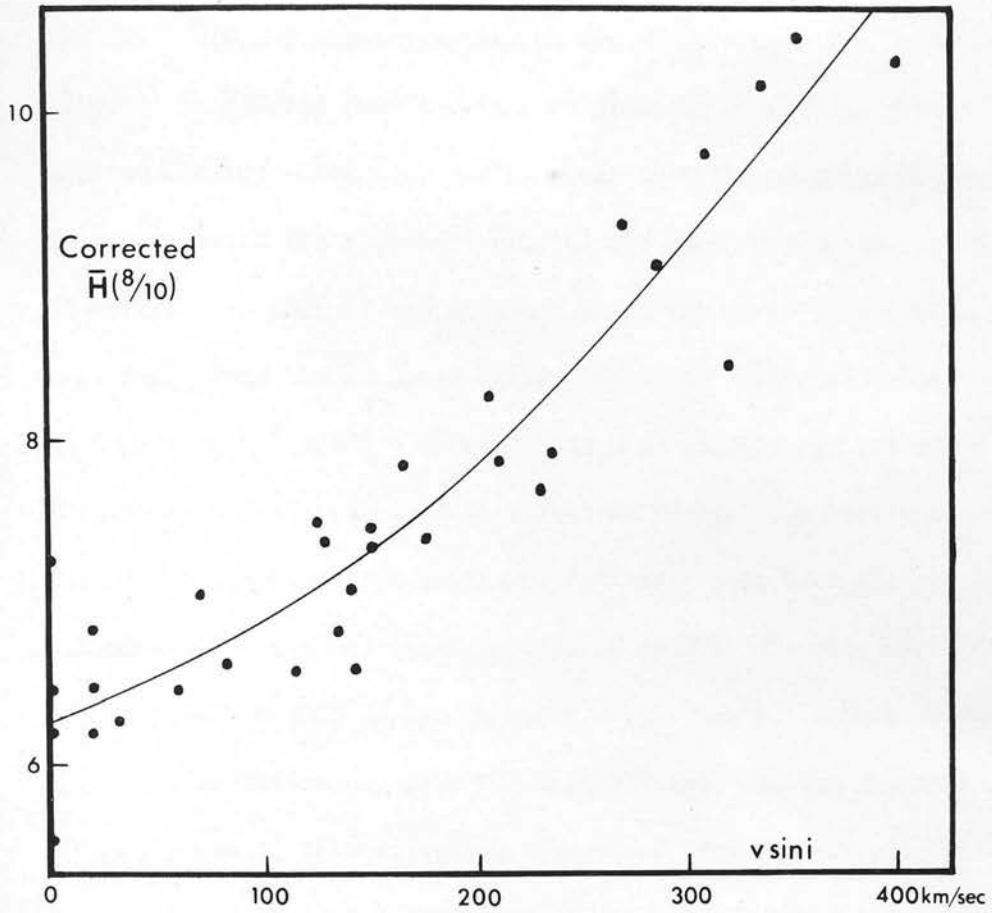


Figure 4

RELATION BETWEEN THE DEVIATIONS  $\delta \bar{H}(8/10)$  IN  $\bar{H}(8/10)$   
AND  $\bar{H}(4/10) - \bar{H}(8/10)$ .

Table 1 (continued)

HD	Name	MK	vsini	Group	$\bar{H}$ at 4/10 total depth	$\bar{H}$ at 8/10 total depth	$\bar{HeI}$	Width of Mg 4481
93427	HR4215	B9V*		field	27.7	9.6		
95418	$\beta$ UMa	A1V	32	standard	26.9	7.5		5.2
98664	$\sigma$ Leo	B9V	70	standard	21.5	7.4		5.2
103287	$\gamma$ UMa	A0V	165	standard	26.4	8.8		
110411	$\rho$ Vir	A0V	175	standard	30.5	8.8		
113797	14 CVn	B9V		field	22.4	8.3		
115612	HR5018	B9V*		field	24.9	9.1		
120315	$\eta$ UMa	B3V	210	standard	22.8	8.3	10.4	
130109	109 Vir	A0V	335	standard	28.7	11.1		
138749	$\theta$ CrB	B7m	400	standard	22.5	10.2	13.0	
146926	19 UMi	B8V*		field	21.3	8.6		
147394	$\tau$ Her	B5IV	20	standard	18.9	6.4	7.2	5.0
149630	$\sigma$ Her	B9V	285	standard	23.3	9.4		
155763	$\zeta$ Dra	B6III	20	standard	16.7	5.7	6.3	5.5
160762	$\iota$ Her	B3V	0	standard	16.2	6.3	6.9	5.7
161573		B3V*		IC4665	19.0	6.3	7.9	
161603		B6V*		IC4665	21.5	8.0		
161677		B5V*		IC4665	22.6	10.5		
167965	HR6845	B6V:	235	standard	23.2	8.4		
177003	HR7210	B3V	0	standard	19.2	6.3	7.4	
177410	HR7224	B9V*		field	20.5	7.4		4.3
186882	$\delta$ Cyg	B9.5IIII28		standard	22.1	7.8		9.4
188665	23Cyg	B5V	150	standard	20.6	7.5	8.4	
192907	$\kappa$ Cep	B9III	0	standard	20.6	6.0		6.6
203467	$\epsilon$ Cep	B3V	150	standard	18.2	7.0	9.3	



is labelled with the value of the difference between the width at 4/10 of the total depth and the width at 8/10 of the total depth. This difference  $\bar{H}(4/10) - \bar{H}(8/10)$  depends mainly on the Stark broadening. The deviations  $\delta\bar{H}(8/10)$  in  $\bar{H}(8/10)$  from the mean relation in Fig. 3 are plotted in Fig. 4 against  $\bar{H}(4/10) - \bar{H}(8/10)$ . It is clear that the relation in Fig. 4 can be used to correct the values of  $\bar{H}(8/10)$  for Stark broadening in the determination of  $v_{\text{ sini}}$ . For each of the standard stars the correction  $-\delta\bar{H}(8/10)$  has been found from the measured value of  $\bar{H}(4/10) - \bar{H}(8/10)$  using the relation in Fig. 4, and  $\bar{H}(8/10) - \delta\bar{H}(8/10)$  has been plotted against  $v_{\text{ sini}}$  in Fig. 5. The standard deviation is  $\pm 44$  km/sec in  $v_{\text{ sini}}$ . The mean widths  $\overline{HeI}$  of the helium lines and the widths of MgII 4481 have been plotted for the standard stars against  $v_{\text{ sini}}$  in Figs. 6 and 7. The standard deviations are  $\pm 33$  km/sec and  $\pm 40$  km/sec in  $v_{\text{ sini}}$  respectively. Values of  $v_{\text{ sini}}$  may therefore be determined from the Balmer lines, and the accuracy achieved is comparable to that of values determined from the HeI and MgII 4481 lines. It should also be noted that if the Balmer lines had not been measured, rotational velocities for 18 of the 50 stars could not have been obtained from spectra of this dispersion and width owing to the weakness of the HeI and MgII 4481 lines. Since the mean error of values of  $v_{\text{ sini}}$  given by Slettebak and Howard is about  $\pm 20$  km/sec, the mean error of the present determinations using all the measured lines will be about  $\pm 35$  km/sec. The standard values of  $v_{\text{ sini}}$  were determined by Slettebak and Howard from line profiles of one lines (HeI 4471 or MgII 4481) from prism spectra taken on IIA0 emulsion at a dispersion of 28A/mm at HV and a width of about 2mm.

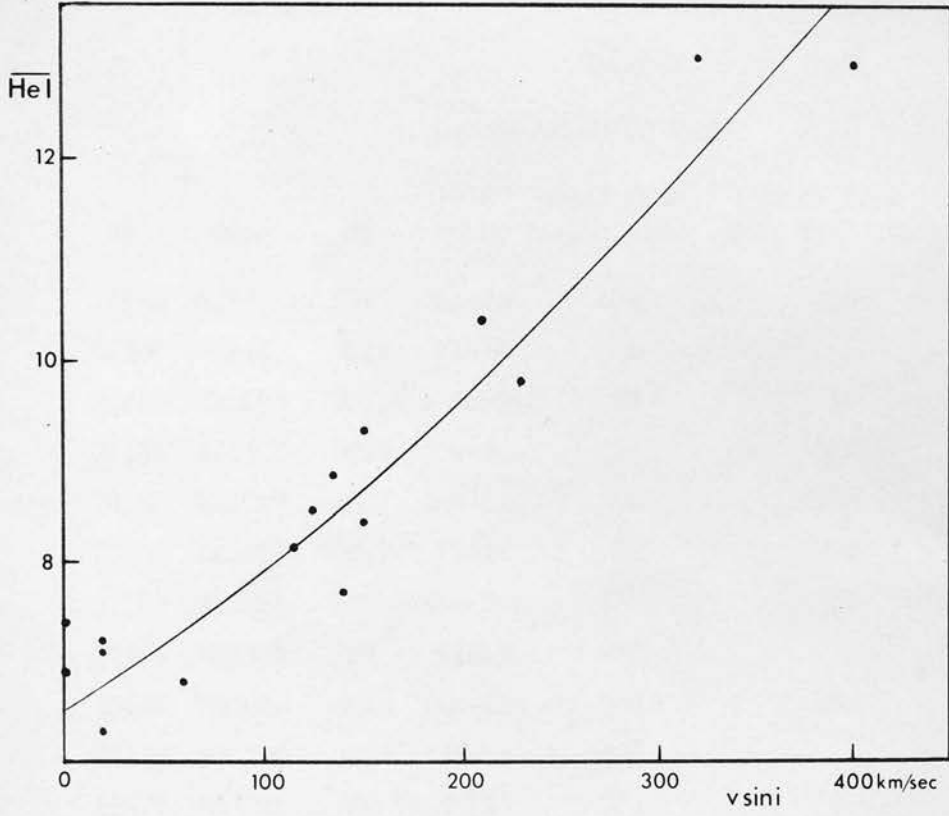


Figure 6

RELATION BETWEEN THE MEAN WIDTHS  $\overline{\text{He I}}$  OF THE  
HELIUM LINES AND  $v \sin i$ .

Allowing for the difference in dispersion and width of the spectra, the accuracy of the present determinations therefore compares very favourably with the accuracy of the standard values. This emphasises the advantage of measuring several lines for each star.

Table 2

## MEASURES OF VSINI

HD	Name	MK	Group	vsini from Balmer lines	vsini from HeI, MgII lines	No. of lines measured	Mean vsini
6300	HR302	B3V	Cas-Tau	170	170	4	170
16004	HR746	B8IV	field	0			0
21661	HR1059	B8III*	$\alpha$ Persei	70	10	1	40
27192	HR1333	B2IV	Cas-Tau	250	160	4	205
34233	HR1719	B3IV	Cas-Tau	80	130	2	105
36881	HR1883	B8III	field	80	0	1	40
37367	HR1924	B2V	Cas-Tau	180	50	4	115
37519	HR1938	B7V	field	270			270
39698	HR2052	B2V	Cas-Tau	220	180	4	200
91130	33 LMi	A0IV	field	100			100
93427	HR4215	B9V*	field	260			260
113797	14 CVn	B9V	field	210			210
115612	HR5018	B9V*	field	240			240
146926	19 UMi	B8V*	field	250			250
161573		B3V*	IC4665	0	100	4	50
161603		B6V*	IC4665	200			200
161677		B5V*	IC4665	390			390
177410	HR7224	B9V*	field	140	0	1	70

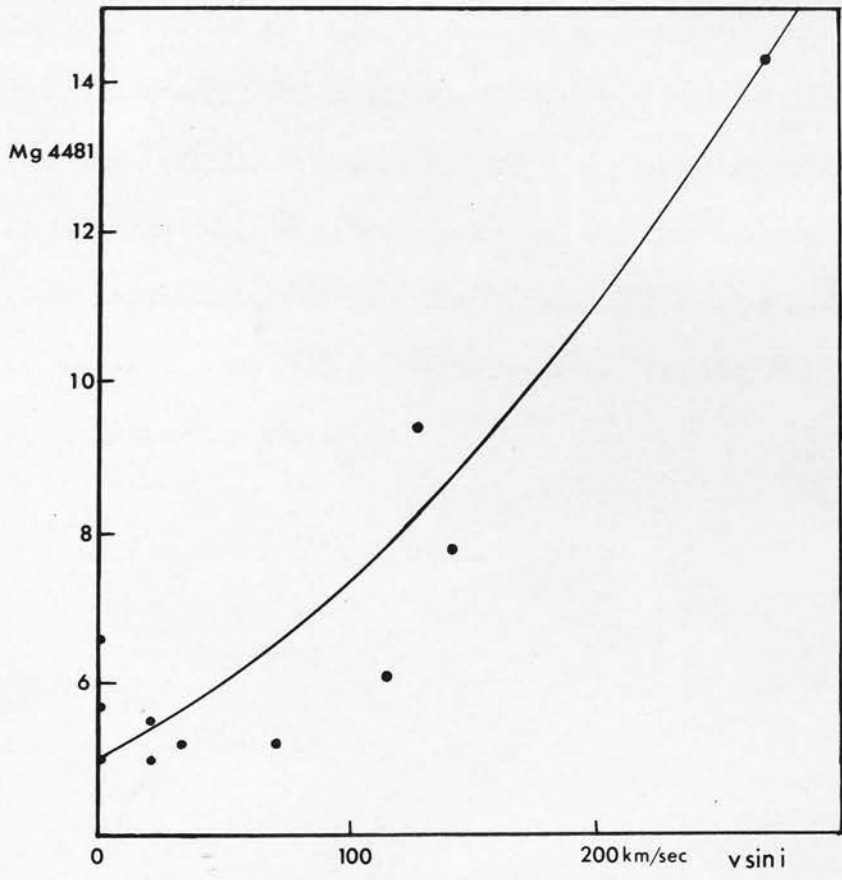


Figure 7

RELATION BETWEEN THE WIDTHS OF Mg 4481 AND VSINI.



The rotational velocities of the 18 stars not included in the lists by Slettebak and Howard have been determined from Figs. 5, 6 and 7, and are listed in Table 2. For every star 5 Balmer lines were measured. The number of He I and MgII lines measured is given after the value of  $v \sin i$  in Table 2. The MK types in Tables 1 and 2 have been taken in most cases from lists by Slettebak (1954), Slettebak and Howard (1955), Blaauw (1956), and Osawa (1959). Other stars have been classified by visual inspection of tracings taken with the Joyce-Loebl microdensitometer with a tracing to plate magnification of 20. The MK types for these stars are followed by an asterisk. The SiIII 4128-4130 blend for the star HR7224 (classified as B9V) is exceptionally strong.

## CHAPTER 5

### AGES AND DISTANCES OF B-TYPE STARS

#### Age determinations from Balmer line intensities

The determination of the ages of stars from their positions in the colour-magnitude diagram is limited to cluster members and nearby stars for which distances are known. For the determination of ages from positions on the  $\beta - (U - B)_0$  diagram, however, it is not necessary to know the distances of the stars, and this method may therefore be extended to B-type stars which are not cluster members. In addition, for B-type stars, the effect of multiplicity on position in the  $\beta - (U - B)_0$  diagram is much smaller than in the colour-magnitude diagram (Crawford, 1958). Rotation affects the positions in both diagrams; the discussion in Chapter 2 shows that it is possible to correct for rotation in the  $\beta - (U - B)_0$  diagram, but it is not possible to correct for rotation in the colour-magnitude diagram unless the inclination of the axis of rotation is known (Sweet and Roy, 1953).

Since the mean slope of the deviations is 0.00017 in  $\bar{\beta}$  per km/sec in  $v \sin i$ , a correction for rotation may be applied by plotting  $\bar{\beta} + 0.00017v \sin i$  against  $(U - B)_0$ . This has been done in Fig. 1 for the Pleiades and  $\alpha$  Persei clusters and the Orion association and for the II Per, I Lac and the II Sco associations which are now discussed.

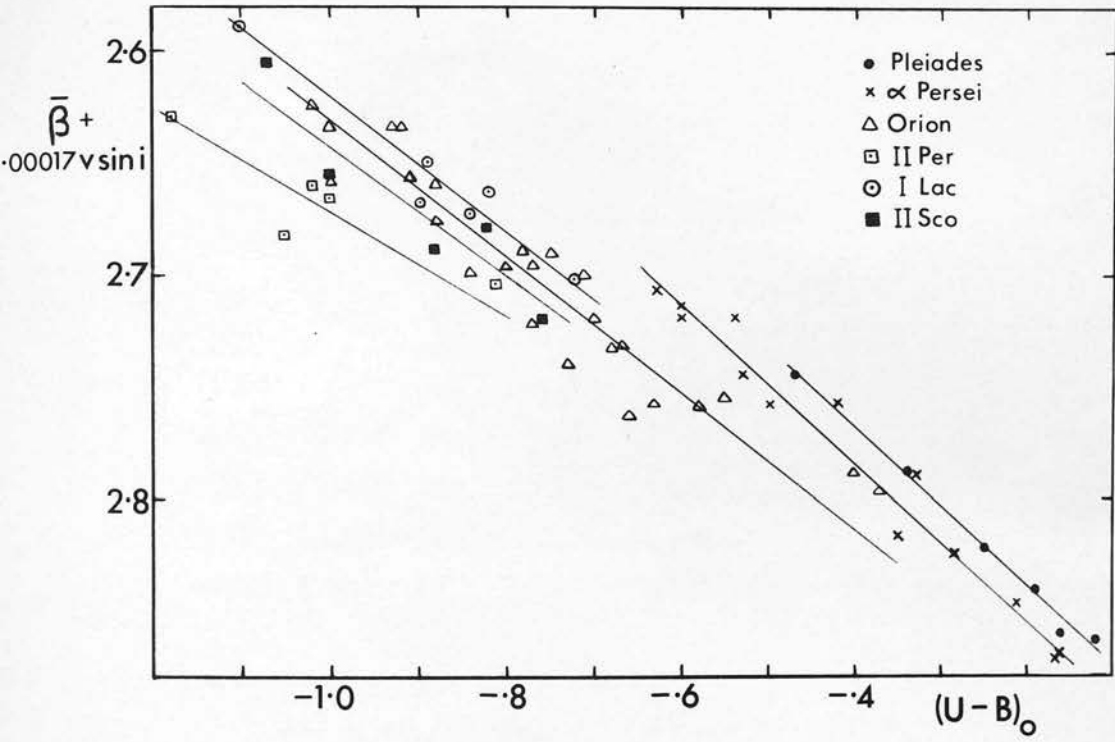


Figure 1

$\bar{\beta} - (U - B)_0$  DIAGRAM CORRECTED FOR ROTATION.

(i) II Per association. The UBV photometry by Harris (1956) has been used.  $\bar{\beta}$  has been found by averaging the  $\beta$  measures by Crawford (1958) and the  $\Gamma$  measures by Bappu et al. (1962) transformed to Crawford's system. The values of vsini are from Treanor (1960) or Slettebak (1949). HD 24640 is variable (Jones, 1960), and has been omitted.

Table 1

## II PER ASSOCIATION

HD	Name	MK	$(U - B)_0$	$\beta$	Transformed $\Gamma$	$\bar{\beta}$	vsini	$\bar{\beta} + 0.00017vsini$
21856		B1V	-1.02	2.634	2.632	2.633	150	2.659
22951	40 Per	B0.5V	-1.05		2.660	2.660	130	2.682
23625	HRL163	B2V	-0.81	2.664	2.683	2.674	170	2.703
24131	HRL191	B1V	-1.00	2.632	2.650	2.641	140	2.665
24912	5 Per	O7	-1.18	2.581	2.596	2.588	240	2.629

(ii) I Lac association. The UBV photometry by Harris (1955), the  $\beta$  measures by Crawford (1961), and the values of vsini by Abt and Hunter (1962) have been used. Only stars in the central region (Table 1 by Crawford) have been included; the stars in the dispersed outer region are older.

Table 2

## I LAC ASSOCIATION

HD	BD	Name	MK	$(U - B)_0$	$\beta$	vsini	$\beta + 0.00017vsini$
212978	39 <sup>0</sup> 4841	HR8553	B2V	-.82	2.642	115	2.662
213976	40 4854		B1.5V	-.90	2.644	135	2.667
214167	38 4808B	8 LacB	B2V	-.89	2.644	30	2.649
214263	37 4631		B2V	-.84	2.651	125	2.672
214432	38 4817		B3V	-.72	2.671	185	2.702
214680	38 4826	10 Lac	O9V	-1.10	2.585	25	2.589

(iii) II Sco association. The UBV photometry and  $\beta$  measures by Hardie and Crawford (1961) have been used. As in previous cases  $(U - B)_0$  has been found by using the nomogram by Johnson (1958).  $\Gamma$  measures by Bappu et al. (1962) have been transformed to Crawford's system. The approximate rotational velocities by Su-Shu Huang (1953) have been used. Hardie and Crawford observed only the northern part of the association.

Table 3

## II SCO ASSOCIATION

HD	Boss No.	MK	$(U - B)_0$	$\beta$	Transformed		vsini	$\bar{\beta} + 0.00017vsini$
					$\Gamma$	$\bar{\beta}$		
141637	4019	B2V	-.88	2.640	2.653	2.646	250	2.688
142669	4052	B2V	-.82	2.648	2.655	2.651	160	2.678
144470	4093	B1V	-1.00	2.623	2.641	2.632	140	2.656
148605	4198	B2V	-.76	2.672	2.664	2.668	300	2.719
149438	4218	B0V	-1.07	2.589	2.621	2.605	0	2.605

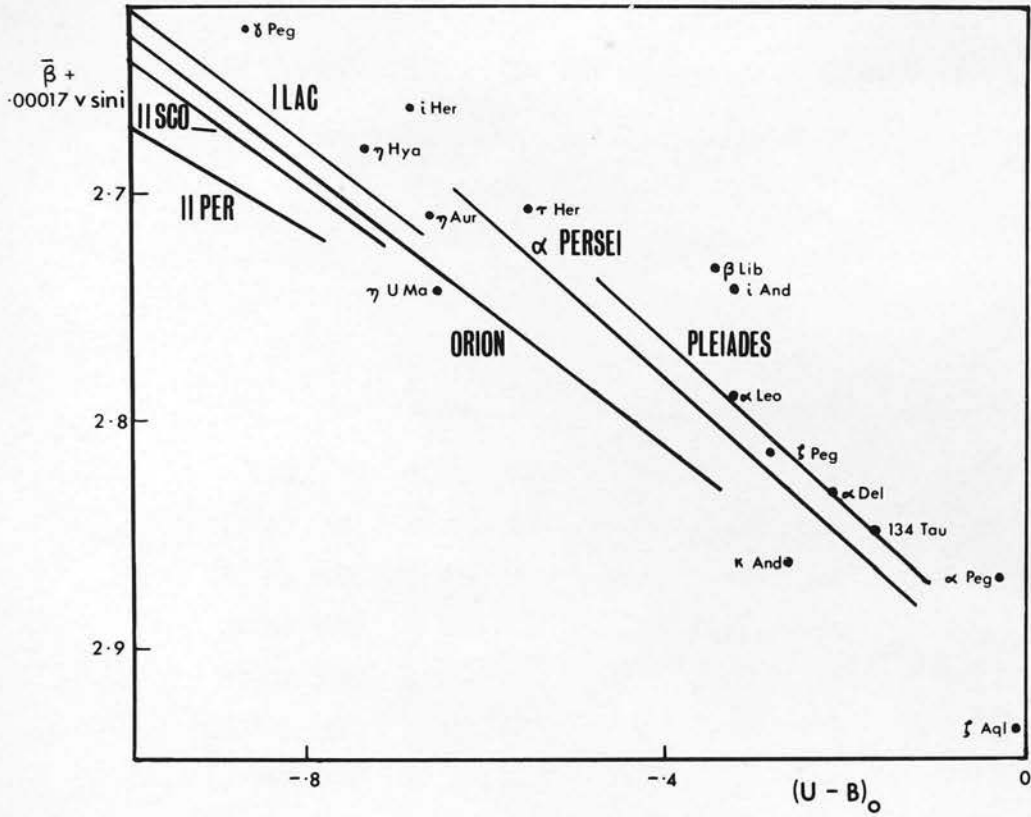


Figure 2

AGES OF FIELD STARS RELATIVE TO CLUSTERS AND ASSOCIATIONS.

The ages of some B-type field stars relative to these clusters and associations are shown in Fig. 2.  $\bar{\beta}$  was calculated from  $\beta$  measures by Crawford (1958, 1960) and  $\Gamma$  measures by Bappu et al. (1962). The values of vsini were taken from Slettebak (1954) or Slettebak and Howard (1955). The UBV photometry by Johnson (1953, 1955) or Eggen (1963) was used. All luminosity class IV and V stars earlier

Table 4

## FIELD STARS

HD	HR	Name	MK	(U - B) <sub>o</sub>	$\bar{\beta}$	vsini	$\bar{\beta} + 0.00017vsini$	(Q - P) <sub>o</sub>
886	39	$\chi$ Peg	B2IV	-.87	2.628	0	2.628	0.073
32630	1641	$\eta$ Aur	B3V	-.67	2.689	125	2.710	0.120
38899	2010	134 Tau	B9IV	-.17	2.848	8	2.849	
74280	3454	$\eta$ Hya	B3V	-.74	2.657	135	2.680	
87901	3982	$\alpha$ Leo	B7V	-.33	2.730	352	2.790	
120315	5191	$\eta$ UMa	B3V	-.66	2.707	210	2.743	0.115
135742	5685	$\beta$ Lib	B8V	-.35	2.695	230	2.734	
147394	6092	$\tau$ Her	B5IV	-.56	2.704	20	2.707	
160762	6588	$\iota$ Her	B3IV	-.69	2.663	0	2.663	
177724	7235	$\zeta$ Aql	B9.5V	-.01	2.876	365	2.938	
196867	7906	$\alpha$ Del	B9V	-.22	2.805	160	2.832	0.323
214923	8634	$\zeta$ Peg	B8V	-.29	2.778	210	2.814	0.315
218045	8781	$\alpha$ Peg	B9V	-.03	2.845	155	2.871	
222173	8965	$\iota$ And	B8V	-.33	2.728	88	2.743	
222439	8976	$\kappa$ And	B8V	-.27	2.831	195	2.864	



than AO with data from these sources were included, with the exception of binary and peculiar stars. The  $H\beta$  photometry by Crawford (1963b) is of lower accuracy, and most of the stars have only one observation. However, seven observations were taken for 134 Tau, and this star has therefore been included.

The approximate ages of the clusters and associations in Fig. 1 may be determined from the spectral type of the earliest main-sequence star according to the relation given by von Hoerner (1957), and the results are given in Table 5. The clusters and associations are listed in the order in which they appear in Fig. 1, and the ages in the last column agree with this order except for the I Lac association.

Table 5

AGES OF CLUSTERS AND ASSOCIATIONS

Association or cluster	Spectral type of earliest main-sequence star	Approximate age ( $10^6$ years)
II Per	O7	1
II Sco	B0	4
Orion (excluding Sword region)	B0.5	5
I Lac	O9	3
$\alpha$ Persei	B3	10
Pleiades	B6	80



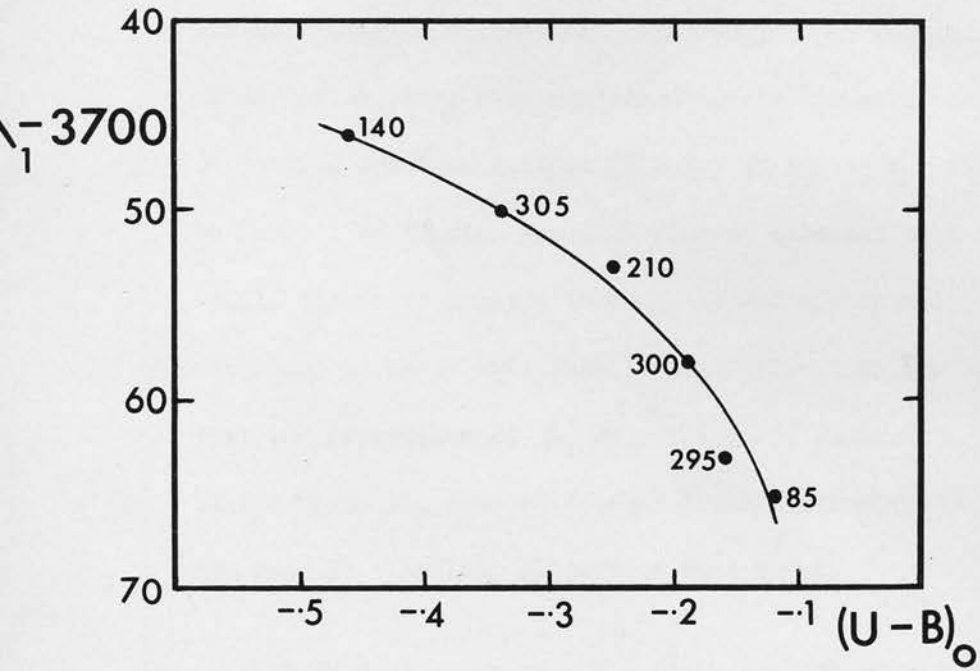


Figure 3  
RELATION BETWEEN  $\lambda_1 - 3700$  AND  $(U - B)_0$  FOR  
THE PLEIADES.

Age determinations from the Balmer discontinuity

Berger (1962) has used measures of the wavelength  $\lambda_1$  and the size D of the Balmer discontinuity for some clusters, associations and binary stars to calibrate the  $\lambda_1 - D$  diagram for age. The positions of the field stars in Fig. 2 agree well with the relative positions on the  $\lambda_1 - D$  diagram. It would be interesting to discover whether rotation affects  $\lambda_1$ . The only suitable cluster for which values of  $\lambda_1$  have been published is the Pleiades (Berger, 1956).  $\lambda_1 - 3700$  has been against  $(U - B)_0$  in Fig. 3 for the stars listed in Table 1 of Chapter 2. Each star is labelled with the value of  $v_{\text{ini}}$ , but there appears to be no dependence on  $v_{\text{ini}}$ . It will be necessary to check this result using other clusters. If it is found that the dependence of  $\lambda_1$  on rotation is small, it will be possible to determine the ages of fainter field stars since  $\lambda_1$  can be measured at a smaller dispersion than  $v_{\text{ini}}$ .

It is well known that the Stark broadening of the higher Balmer lines depresses the continuum in this region and hence increases  $\lambda_1$ . Since the Stark broadening decreases when the effective surface gravity decreases, rotation would be expected to reduce  $\lambda_1$ . A possible explanation of the lack of dependence on rotational velocity of the positions of the Pleiades stars in the  $\lambda_1 - (U - B)_0$  diagram is that the rotational broadening compensates the decrease in Stark broadening due to the lowering of the effective surface gravity in the equatorial

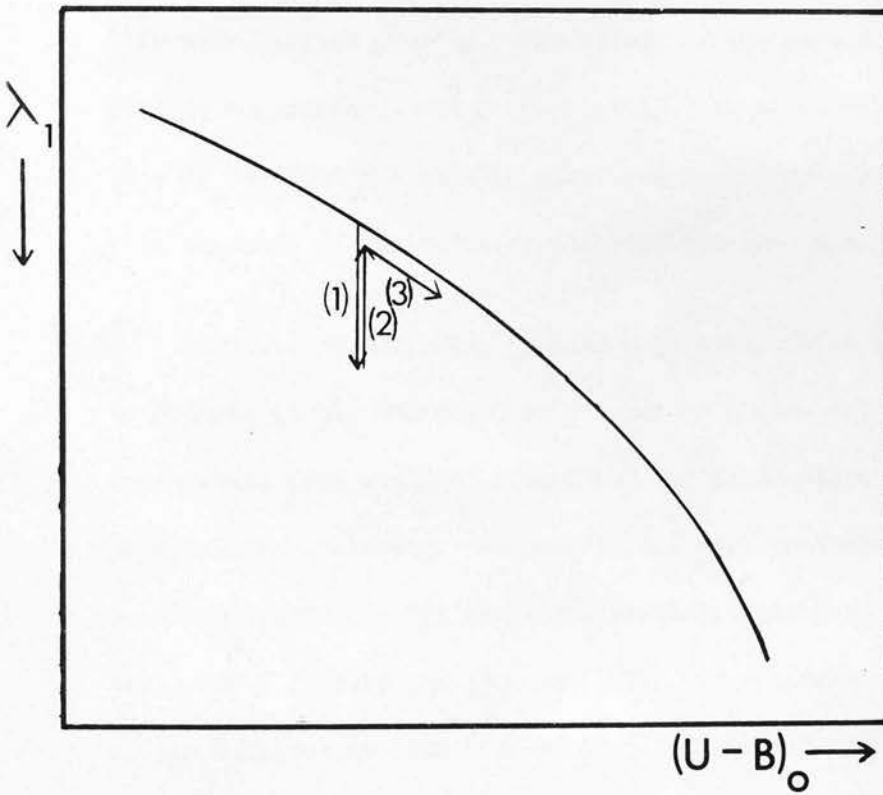


Figure 4  
THE EFFECT OF ROTATION ON THE POSITION OF A STAR  
IN THE  $\lambda_1 - (U - B)_0$  DIAGRAM.

region of the star. Kaler (1962) discussed  $\alpha$  Ophiuchi, a star of spectral type A5 and rotational velocity 220 km/sec; he showed that the rotational broadening increased the observed value of  $\lambda_1$  by about 3A. Fig. 4 shows the effect of rotation on the position of a star on the  $\lambda_1 - (U - B)_0$  diagram. The arrow (1) shows the increase in  $\lambda_1$  due to rotational broadening of the higher Balmer lines, and arrow (2) shows the decrease in  $\lambda_1$  due to the reduction of the effective surface gravity. The effect of the reduction of the apparent surface temperature, shown by arrow (3), is to increase both  $\lambda_1$  and  $(U - B)_0$  so that the star is displaced approximately parallel to the main sequence of non-rotating stars of the same age.

It would be desirable to have a quantity which would be sensitive to changes in  $\lambda_1$  and could be determined photoelectrically, so that approximate ages could be determined for field stars with no measures of rotational velocity. Borgman (1960) made photoelectric measures of a colour index  $(Q - P)$ , where the wavelengths of peak transmission of the Q and P filters are 3560 and 3750A respectively, and the half-width of the P filter is 110A. Crawford (1958) showed that there was a linear relation between  $(U - B)_0$  and D. Hence for a given value of  $(U - B)_0$ ,  $(Q - P)$  will increase as  $\lambda_1$  decreases. Thus an age diagram can be formed by plotting the intrinsic colour index  $(Q - P)_0$  against  $(U - B)_0$ , and this diagram will appear reversed with respect to age compared with the  $\lambda_1 - D$  and  $\beta - (U - B)_0$  diagrams.

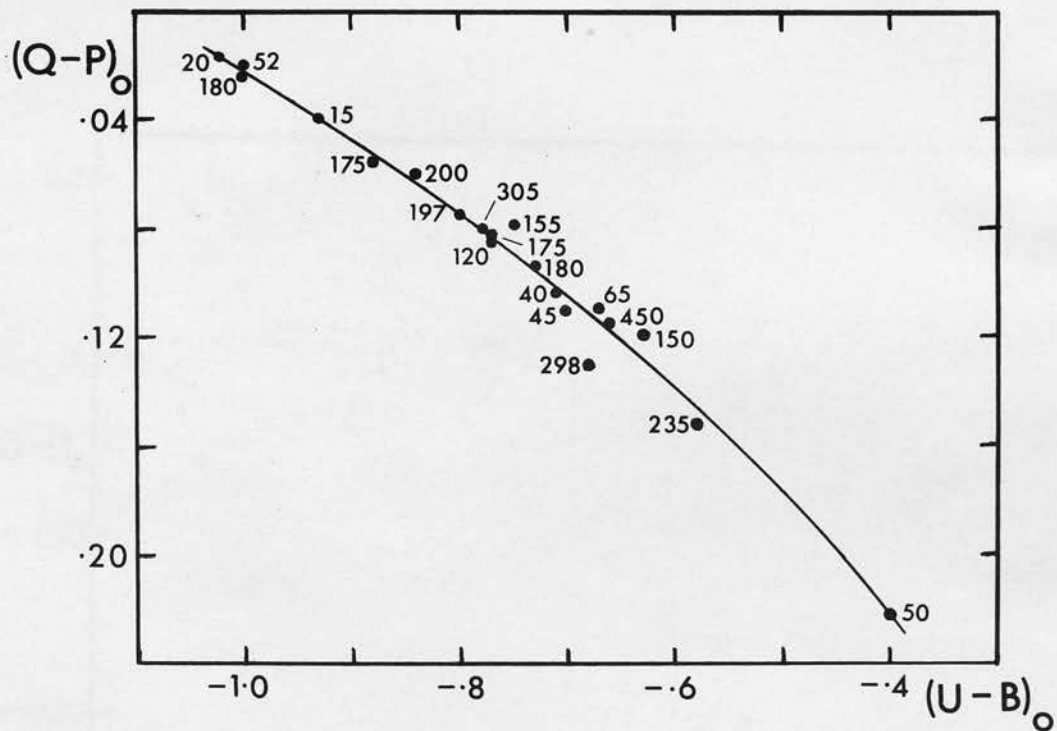


Figure 5  
RELATION BETWEEN  $(Q - P)_0$  AND  $(U - B)_0$   
FOR THE ORION ASSOCIATION.

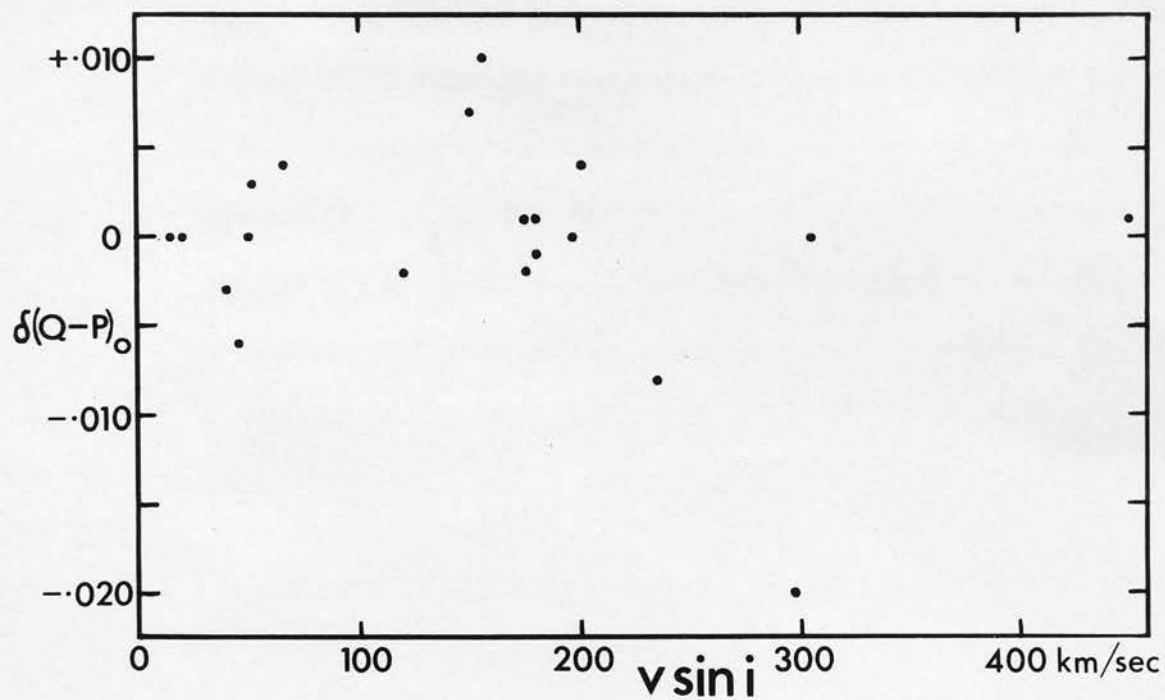


Figure 6

DEVIATIONS IN  $(Q - P)_0$  FOR THE ORION ASSOCIATION.

Borgman has measured  $(Q - P)$  for 20 of the 25 stars in the Orion association listed in Table 3 of Chapter 2. The colour excess  $E_{Q - P}$  has been calculated from the approximate relation

$$E_{Q - P} = 0.25E_{U - B}, \quad (1)$$

and hence the values of  $(Q - P)_0$  given in this table have been obtained. Equation (1) has been derived from the effective wavelengths of the filters U and B and the wavelengths of peak transmission of the filters Q and P assuming a  $1/\lambda$  reddening law.  $(Q - P)_0$  has been plotted against  $(U - B)_0$  in Fig. 5. The deviations  $\delta(Q - P)_0$  have been plotted against  $v \sin i$  in Fig. 6, and it appears that there is no significant dependence of the deviations on  $v \sin i$ . It should be noted that the discussion of the dependence of  $\lambda_1$  on rotation does not apply directly to  $(Q - P)_0$ , since the P filter includes both continuum and lines.

The values of  $(Q - P)_0$  for the stars in Tables 1 and 3 in the II Per and II Sco associations are listed in Table 6, and have been plotted against  $(U - B)_0$  in Fig. 7. The positions of the field stars with  $(Q - P)_0$  values in Table 4 are also given. It is apparent that the stars in the II Per and II Sco associations are less evolved than those in the Orion association. This agrees with the relative ages of these associations in the plot of  $\bar{\beta} + 0.00017v \sin i$  against  $(U - B)_0$  in Fig. 1. There is also good agreement between the relative positions of the field stars in Fig. 7 and those in Fig. 2. Since one age

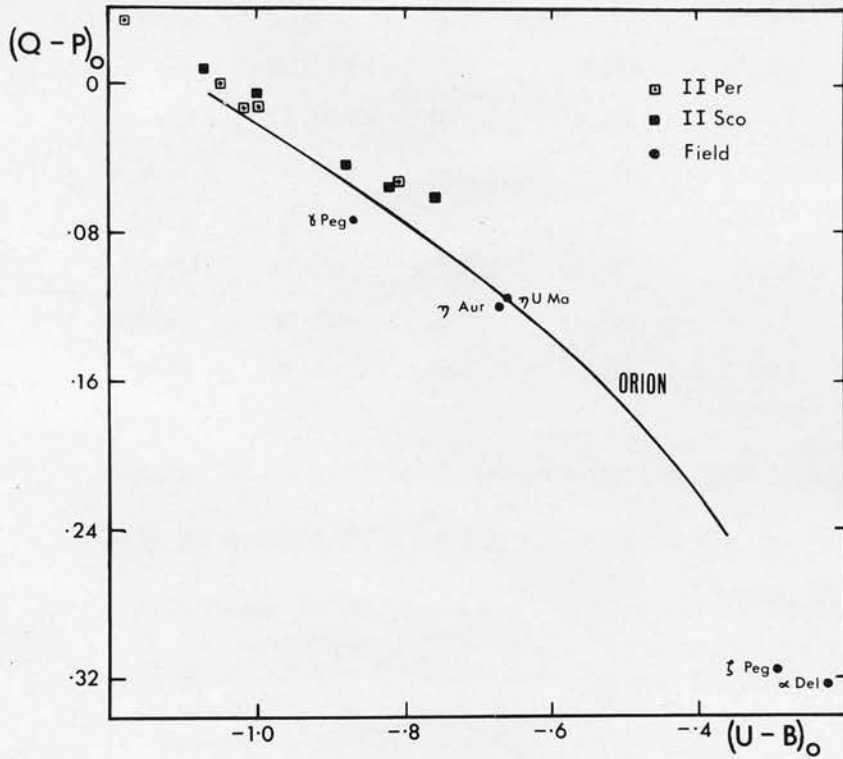


Figure 7  
AGES OF STARS COMPARED WITH THE AGE OF THE  
ORION ASSOCIATION.



Table 6

VALUES OF  $(Q - P)_0$ 

HD	Name	MK	$(U - B)$	$(U - B)_0$	$(Q - P)$	$(Q - P)_0$
21856		B1V	-0.85	-1.02	0.056	0.013
22951	40 Per	B0.5V	-0.84	-1.05	0.053	0.000
23625	HR1163	B2V	-0.60	-0.81	0.106	0.053
24131	HR1191	B1V	-0.80	-1.00	0.062	0.012
24912	$\xi$ Per	O7	-0.92	-1.18	0.031	-0.034
141637	1 Sco	B2V	-0.72	-0.88	0.084	0.044
142669	$\rho$ ScoA	B2V	-0.82	-0.82	0.056	0.056
144470	$\omega'$ Sco	B1V	-0.83	-1.00	0.048	0.005
148605	22 Sco	B2V	-0.70	-0.76	0.076	0.061
149438	$\tau$ Sco	B0V	-1.04	-1.07	-0.001	-0.009

diagram is reversed with respect to the other, any error in  $(U - B)_0$  will be doubled in a comparison between the two diagrams. The age effect seems to be smaller in Fig. 7, and it is suggested that if the half-width of the P filter was reduced,  $(Q - P)_0$  would be more sensitive to changes in effective surface gravity and a better age diagram would result. If the half-width and effective wavelength of the P filter were chosen so that it measured the continuum between two of the higher Balmer lines, this age diagram would also have only a small dependence on rotation according to the discussion given for  $\lambda_1$ .

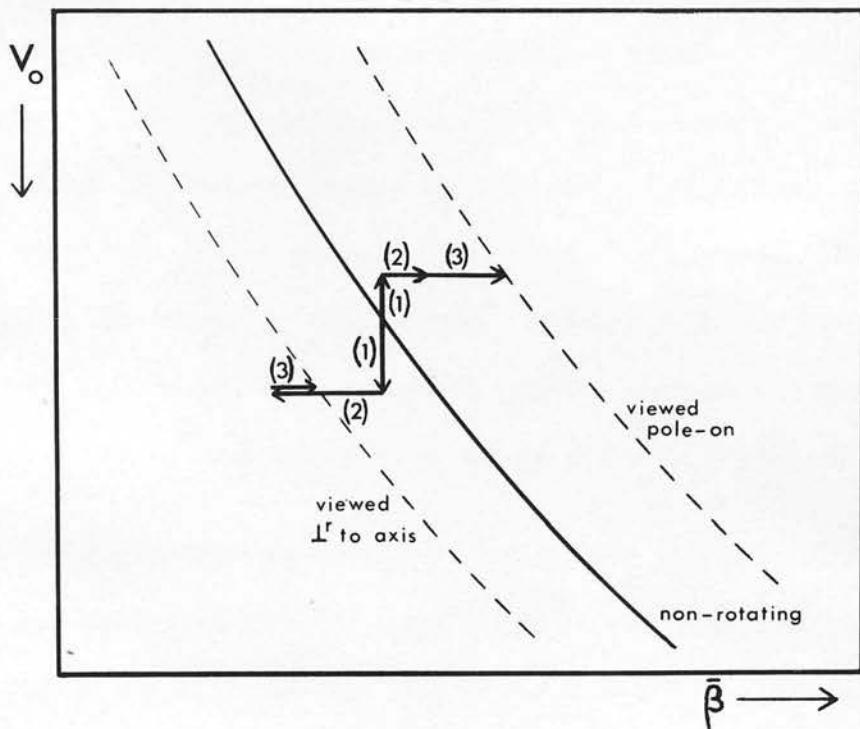


Figure 8

THE EFFECT OF ROTATION ON THE POSITION OF A STAR  
IN THE  $V_0 - \bar{\beta}$  DIAGRAM.

Determination of the inclinations of the axes of rotation

Sweet and Roy (1953) showed that the apparent luminosity is reduced when a star is viewed perpendicular to the axis of rotation and increased when it is viewed pole-on; the apparent surface temperature is reduced in both cases. They concluded that no definite separation of cluster stars according to rotation could be obtained in the H-R diagram. However, Fig. 8 shows that a plot of  $V_0$ , the visual magnitude corrected for interstellar absorption, against  $\bar{\beta}$  separates cluster stars of high and low inclinations. The arrows (1) show the effect of the changes in luminosity on  $V_0$ . The effect of the changes in effective surface gravity and apparent surface temperature on  $\bar{\beta}$  are shown by arrows (2) and (3) respectively.

An attempt has been made in Fig. 9 to recognise stars of high and low inclinations in the  $\alpha$  Persei cluster using the values of  $\bar{\beta}$  and  $V_0$  given in Table 7. The colour excess  $E_B - V$  has been determined using Johnson's nomogram, and  $V_0$  has been calculated taking 3.0 as the ratio of the total to selective absorption. It is clear from Fig. 8 that for a given value of  $v \sin i$  stars with high values of inclination  $i$  will lie below and to the left of stars with low values of  $i$ . Thus, for example, HD 21071 with  $v \sin i = 70$  lies below and to the left of the mean relation between  $V_0$  and  $\bar{\beta}$ , while HD 21278 with  $v \sin i = 63$  lies above and to the right of the relation. HD 21071 therefore has a higher value of  $i$  than HD 21278.  $\bar{\beta}$  for HD 22136 is

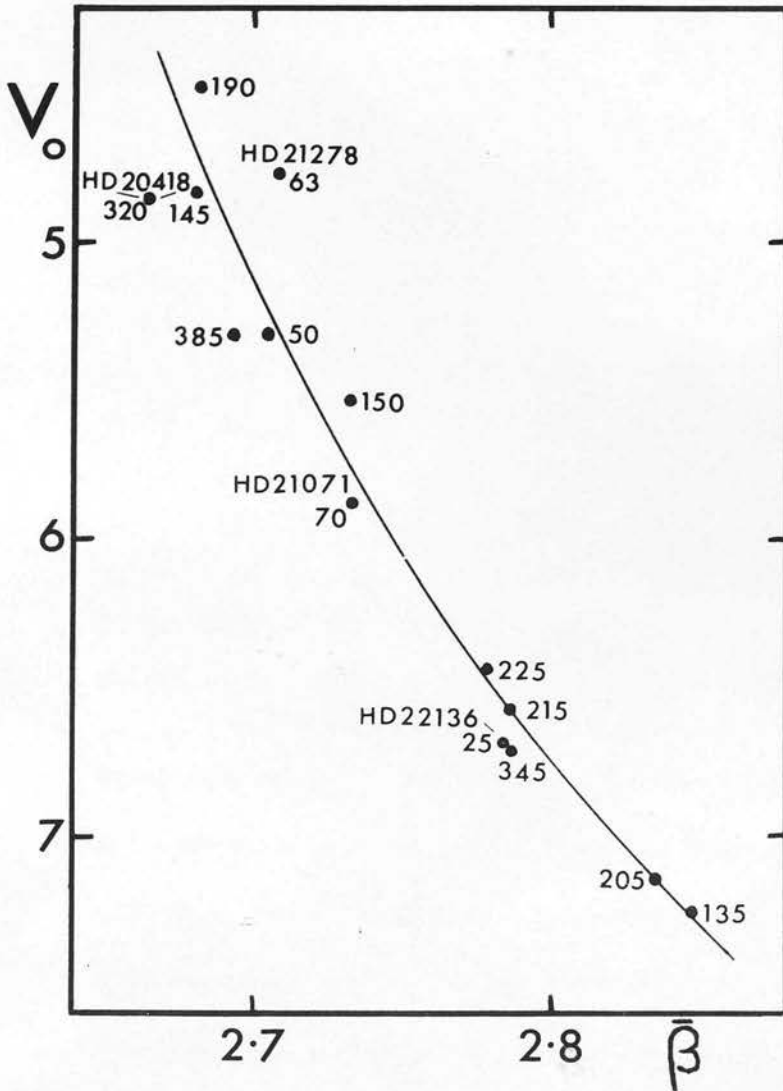


Figure 9

$V_0 - \bar{\beta}$  DIAGRAM FOR THE  $\alpha$  PERSEI CLUSTER.

Table 7

 $\alpha$  PERSEI CLUSTER

HD	Mitchell	MK	$\bar{\beta}$	vsini	$V_o$	$M_v$
	No.					
20365	383	B3V	2.680	145	4.83	-1.27
20418	401	B5V	2.664	320	4.85	-1.25
21071	675	B6V	2.733	70	5.88	-0.22
21181	735	B9V	2.787	345	6.71	0.61
21278	774	B3V	2.708	63	4.77	-1.33
21362	810	B6V	2.693	385	5.31	-0.79
21398	831	B9V	2.848	135	7.25	1.15
21428	835	B5V	2.681	190	4.48	-1.62
21455	861	B5V	2.732	150	5.53	-0.57
21641	955	B9V	2.786	215	6.57	0.47
21672	965	B8V	2.779	225	6.43	0.33
21699	985	B8III	2.705	50	5.31	-0.79
21931	1082	B9V	2.835	205	7.14	1.04
22136	1153	B8V	2.785	25	6.68	0.58

based only on photographic measures, but its position in Fig. 9 would indicate that it could not be a rapidly rotating pole-on star. HD 20418 with  $vsini = 320$  km/sec has a high value of  $\bar{\beta}$ ; this may be inferred both from its position in Fig. 9 and from the fact that if its equatorial velocity were much greater than 320 km/sec, it would be an emission-line star. These conclusions might be affected if binaries and non-members have been accidentally included.

The standard deviation in  $V_o$  in Fig. 9 is  $\pm 0.26^m$ . The mean error

in  $\bar{\beta}$  is  $\pm 0.006$  corresponding to  $\pm 0.10^m$  in  $V_o$ . The approximate mean error in  $V_o$  is  $\pm 0.05^m$ . This leaves a dispersion of  $\pm 0.23^m$  unaccounted for. In a similar analysis on the II Sco association Hardie and Crawford (1961) found a "cosmic dispersion" of  $\pm 0.26^m$ . The mean value of  $v_o$  for B5V stars is about 200 km/sec (Slettebak and Howard, 1955). For a star viewed perpendicular to the axis of rotation, the lowering of the effective surface gravity gives an observed decrease in  $\bar{\beta}$  of 0.034. Sweet and Roy give the reduction in  $\log T_e$  as  $0.065 \alpha_1$ , which corresponds to an increase in  $\bar{\beta}$  of 0.007 according to Sinnerstad's diagram. The combined result is a decrease in  $\bar{\beta}$  of 0.027, which corresponds to an increase of  $0.54^m$  in  $V_o$  on Fig. 9 in the region of B5 stars. There is an increase in the bolometric magnitude  $M_{bol}$  of  $0.569 \alpha_1$  (Sweet and Roy, 1953); applying the bolometric correction, this gives an increase in  $V_o$  of  $0.08^m$ . Hence the total deviation is  $0.62^m$  in  $V_o$ . Similarly, for a B5V star viewed pole-on, the predicted increase in  $\bar{\beta}$  due to the increase in effective surface gravity is 0.002, and the increase in  $\bar{\beta}$  due to the reduction in  $\log T_e$  of  $0.040 \alpha_1$  is 0.005. This gives a total increase in  $\bar{\beta}$  of 0.007 corresponding to a decrease in  $V_o$  of  $0.13^m$ . The decrease in  $M_{bol}$  is  $0.427 \alpha_1$ , which results in a decrease in  $V_o$  of  $0.06^m$ . Thus the total deviation in  $V_o$  is  $0.19^m$ . A large part of the "cosmic dispersion" is therefore caused by rotation.

A possible method of recognising rapidly rotating pole-on stars is suggested by the analysis by Su-Shu Huang and Struve (1956) of Maia (20 Tau),

which is the only B-type star in the Pleiades with a small value of  $v \sin i$  (33 km/sec). They observed lines in its spectrum corresponding to a large range in temperature and suggested that it was a rapidly rotating pole-on star. The high temperatures would occur at the central region of the stellar disc and the low temperatures at the limb according to this explanation. Babcock (1960) has suggested that peculiar A-type stars are rapidly rotating stars observed pole-on.

McNamara and Larsson (1962) noted that three of the stars in the Orion association with low values of  $v \sin i$  (HD 36629, HD 37058, and HD 37807) had weak helium lines for the spectral types derived from  $(U - B)_0$ , but they offered no explanation. The only other peculiarity was the presence of the TiII 3759 and TiII 3761 lines in the spectrum of HD 37058. This line normally appears only in stars later than B8, but the spectral type of this star derived from UBV photometry was B3. If the star is binary, about 1/3 of the light would have to come from a companion star of spectral type about A0 to produce a noticeable weakening of the helium lines. The remaining 2/3 of the light would then have to come from an O-type star to produce the observed value of  $(U - B)_0$ , but McNamara and Larsson did not observe any O-type features at a dispersion of 10.2 Å/mm. It is therefore necessary to postulate a triple star with components of spectral types B2, B6, and A0 approximately, all three components being non-rotating or observed pole-on. The plane of the orbits would have to be perpendicular to the line of sight,



otherwise line doubling would be observed (or at least the measured value of  $v_{\text{ini}}$  would be increased). A more likely explanation is that HD 37058 is a single star which is rapidly rotating and observed pole-on. The helium lines would be produced in the central part of the disc with temperatures corresponding to spectral types earlier than B6. The intermediate zone would have temperatures corresponding to types B6 to B8 and would therefore contribute little to the helium lines. The TiII lines would be formed in the outer zone which would have temperatures corresponding to types later than B8. The observed helium lines are weak, since they are produced in only part of the disc. The TiII lines are stronger in supergiants than in dwarfs; this supports the rotation hypothesis, since the surface gravity of the outer zone would be low.

Morgan, Keenan and Kellman (1943) observed that  $\epsilon$  Cas had weak helium lines. The spectrophotometry by Butler and Seddon (1959) confirmed this. An examination of their results shows that the two B3 stars out of 25 with the weakest lines of CII 4267 are  $\epsilon$  Cas and 42 Cam. The variation of the intensity of CII 4267 with spectral type is similar to that of the helium lines. Slettebak and Howard (1955) used  $\epsilon$  Cas as a standard for rotational velocity measurements and obtained a value of 10 km/sec for  $v_{\text{ini}}$  from the profile of HeI 4471. However, Elvey (1930) obtained a value of 37 km/sec from the profile of MgII 4481. If further observations confirm this difference, it might be accounted for if the star is rapidly rotating and observed pole-on, since the MgII 4481 line would be formed



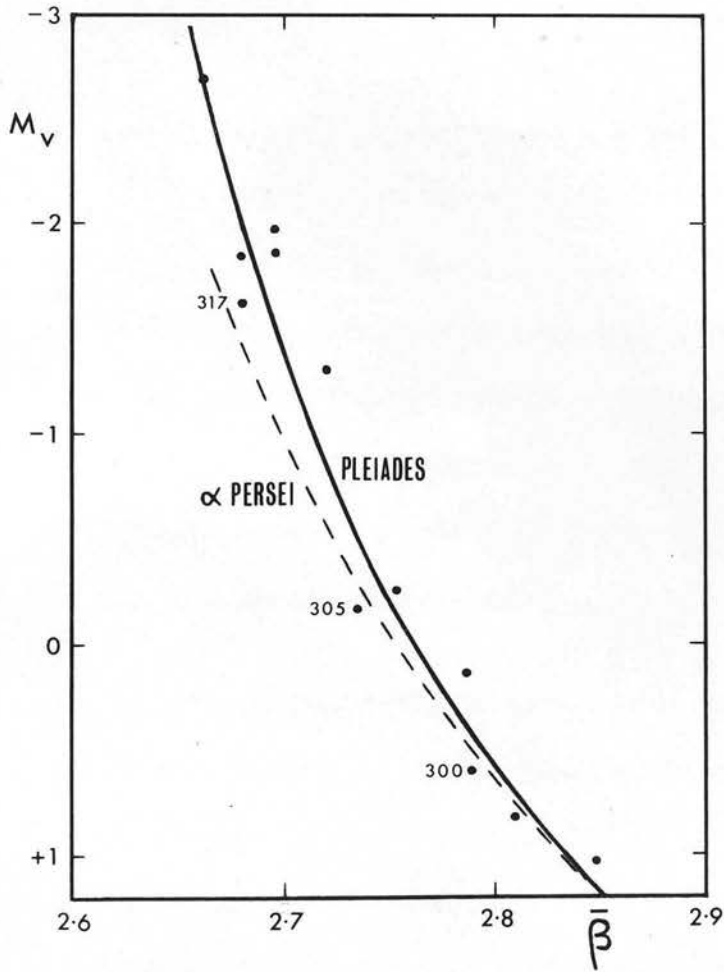


Figure 10  
RELATIONS BETWEEN  $M_V$  AND  $\bar{\beta}$  FOR THE PLEIADES  
AND  $\alpha$  PERSEI CLUSTERS.

predominantly in the outer regions of the disc while the HeI 4471 line would be formed in the central zone. No reference to the ultra-violet spectrum of  $\epsilon$  Cas has been found to check for the presence of the TiII lines.

#### Determination of absolute magnitudes and distances

Since at present there appears to be no general method of determining the inclinations of field stars, rotation imposes a fundamental limit on the accuracy of absolute magnitudes  $M_V$  deduced from Balmer line intensities. However, stars with  $v \sin i \geq 300$  km/sec which are not emission-line stars will have high values of the inclination  $i$ , and should therefore lie below and to the left of the mean relation between  $M_V$  and  $\bar{\beta}$ . This enables a correction for rotation to be applied for these stars.

Evolutionary deviation curves have been plotted for the Pleiades and  $\alpha$  Persei clusters as described by Johnson (1960), and the distance moduli have been found to be  $5.55^m$  and  $6.1^m$  respectively. Table 8 gives the values of  $\bar{\beta}$ ,  $V_0$ , and  $M_V$  for single stars earlier than A0 in the Pleiades.  $M_V$  has been plotted against  $\bar{\beta}$  in Fig. 10. Several of the brightest stars in the Pleiades show a tendency to have emission, and HD 23302, HD 23480, and HD 23630 are included in the catalogue of stars with H $\alpha$  emission given by Merrill and Burwell (1933). As expected, all the stars with  $v \sin i \geq 300$  km/sec in the  $\alpha$  Persei and Pleiades clusters lie below and to the left of the mean relations between  $V_0$  or  $M_V$  and  $\bar{\beta}$ .

Table 8

## PLEIADES

HD	Name	Hertzsprung		$\bar{\beta}$	vsini	$V_0$	$M_V$
		No.	MK				
23288	16 Tau	117	B7IV	2.753	235	5.29	-.26
23302	17 Tau	126	B6III	2.696	237	3.69	-1.86
23338	19 Tau	156	B6V	2.720	140	4.24	-1.31
23408	20 Tau	242	B7III	2.680	33	3.71	-1.84
23432	21 Tau	255	B8V	2.786	210	5.68	+1.13
23441	22 Tau	265	B9V	2.810	295	6.37	+1.82
23480	23 Tau	323	B6IV	2.680	317	3.93	-1.62
23630	$\gamma$ Tau	542	B7III	2.662	213	2.86	-2.69
23753	HR1172	722	B8V	2.735	305	5.38	-.17
23850	27 Tau	870	B8III	2.698	173	3.58	-1.97
23873		910	B9.5V	2.848	85	6.58	+1.03
23923	HR1183	977	B9V	2.789	300	6.15	+1.60

shown in Figs. 9 and 10. The average deviation from the mean relations for these six stars is  $0.33^m$ . The relation between  $M_V$  and  $\bar{\beta}$  for the  $\alpha$  Persei cluster is given by the dotted line in Fig. 10 for comparison with the relation for the Pleiades. The difference between the two relations is largest for the stars of greatest luminosity; this suggests that the difference between the two relations is due to the difference in the ages of the clusters.

Fig. 10 may be regarded as a preliminary calibration for determining the absolute magnitudes of single stars with ages comparable to those

of the  $\alpha$  Persei and Pleiades clusters. A correction of  $0.33^m$  is necessary for stars with  $v \sin i \geq 300$  km/sec. Absolute magnitudes for eight of the field stars shown in Fig. 2 are given in Table 9. The relation between  $M_V$  and  $\bar{\beta}$  for the Pleiades has been used for 134 Tau,  $\alpha$  Leo, and  $\alpha$  Del, while for  $\eta$  Aur,  $\eta$  Hya, and  $i$  Her the relation for the  $\alpha$  Persei cluster has been used. The means of the values given by the two relations have been taken for  $\tau$  Her and  $\zeta$  Peg. The distance moduli  $V_0 - M_V$  and the distances  $d$  in parsecs have also been calculated.

Table 9

## ABSOLUTE MAGNITUDES AND DISTANCES OF FIELD STARS

HD	Name	MK	$\bar{\beta}$	$M_V$	$V_0$	$V_0 - M_V$	$d$
32630	$\eta$ Aur	B3V	2.689	-1.2	3.2	4.4	76
38899	134Tau	B9IV	2.848	+1.2	4.9	3.7	55
74280	$\eta$ Hya	B3V	2.657	-2.0	4.3	6.3	182
87901	$\alpha$ Leo	B7V	2.730	-0.3	1.4	1.7	22
147394	$\tau$ Her	B5IV	2.704	-1.1	3.9	5.0	100
160762	$i$ Her	B3IV	2.663	-1.8	3.8	5.6	132
196867	$\alpha$ Del	B9V	2.805	+0.6	3.8	3.2	44
214923	$\zeta$ Peg	B8V	2.778	+0.3	3.4	3.1	42

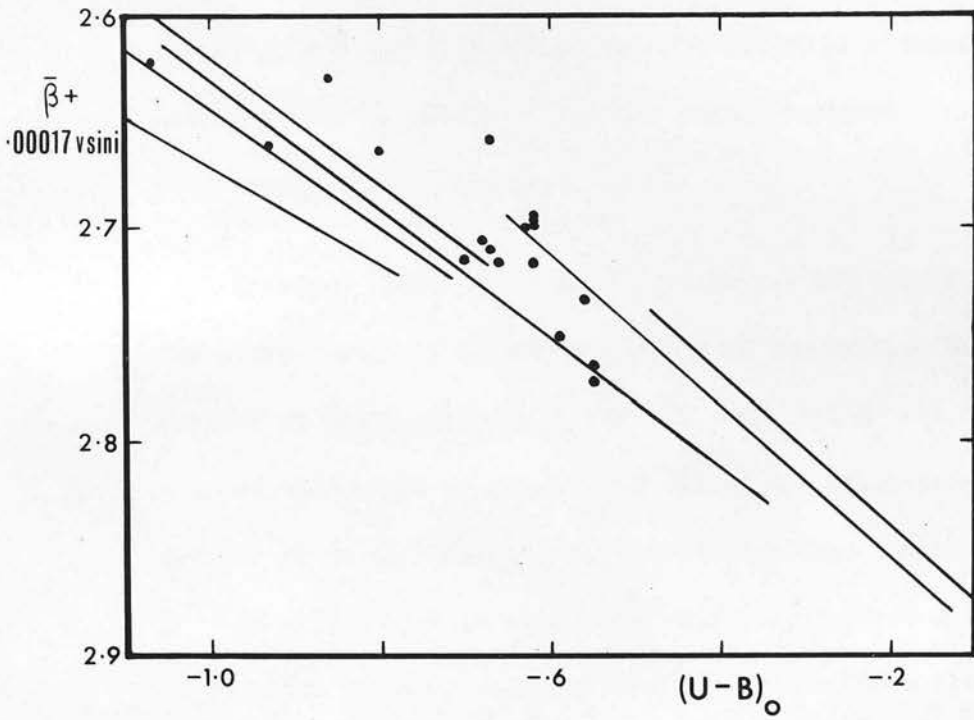


Figure 11

AGES OF STARS IN THE CAS-TAU "GROUP".

Reality of the Cas-Tau "group"

Blaauw (1956) analysed the proper motions of northern O-B5 stars and suggested that many of the brighter stars in the constellations of Cassiopeia and Taurus belonged to a moving cluster. Since this "group" has been used in various absolute magnitude calibrations (e.g. Sinnerstad, 1961) it is important to check its reality. Petrie (1958) showed that the radial velocities and H $\gamma$  intensities could be accounted for by assuming that the stars possessed normal solar motion plus average random motion.

Crawford (1963) obtained photoelectric UB $\gamma$  and H $\beta$  photometry for the stars listed by Blaauw as members of the group. He found that the scatter of these stars in the  $\beta - (U - B)_0$  and  $M_V - \beta$  diagrams was greater than would be expected if all of the stars were members of a group. There is, however, the possibility that the scatter in the  $\beta - (U - B)_0$  might be reduced if only single stars without emission or peculiar features were included, and corrections were applied for rotation. Table 10 gives the data for such stars which have measures of  $v_{\text{sin}i}$  by Slettebak and Howard (1955), Slettebak (1963), or in Table 2 of Chapter 4.  $\bar{\beta} + 0.00017v_{\text{sin}i}$  has been plotted against  $(U - B)_0$  in Fig. 11. The spread in the ages is comparable with that for the field stars shown in Fig. 2. This confirms Crawford's conclusion that either the Cas-Tau group does not exist or most of the stars listed by Blaauw are not members.

Table 10

## CAS-TAU "GROUP"

HD	Name	MK	(U - B) <sub>0</sub>	$\bar{\beta}$	vsini	$\bar{\beta} + 0.00017vsini$
3360	$\zeta$ Cas	B2V	-.86	2.627	20	2.630
3901	$\xi$ Cas	B2V	-.63	2.661	230	2.700
6300		B3V	-.62	2.668	170	2.697
16908	35 Ari	B3V	-.66	2.693	135	2.716
23793	30 Tau	B2IV	-.62	2.692	20	2.695
24760	$\epsilon$ Per	B0.5V	-1.07	2.595	160	2.622
25340	35 Eri	B5V	-.56	2.702	190	2.734
25558	40 Tau	B3V	-.68	2.702	25	2.706
26912	$\mu$ Tau	B3V	-.62	2.685	80	2.699
27192	b <sup>2</sup> Per	B2IV	-.93	2.626	205	2.661
32630	$\eta$ Aur	B3V	-.67	2.689	125	2.710
34233	15 Cam	B3IV	-.55	2.754	105	2.772
35671	115 Tau	B5V	-.59	2.724	160	2.751
35708	114 Tau	B3V	-.80	2.662	10	2.664
36267	32 Ori	B5IV	-.55	2.733	190	2.765
36819	121 Tau	B3V	-.70	2.695	115	2.715
38622	133 Tau	B2V	-.67	2.649	60	2.659
42560	$\xi$ Ori	B3V	-.62	2.677	230	2.716



### CONCLUSIONS

The main conclusion of this investigation is that rotation should be considered in any discussion of B-type stars. Many of the methods at present being used to determine effective temperatures and absolute magnitudes require corrections to take account of the rotation of the stars.

It has been shown that rotation has an important effect on determinations of the relative ages of stars from their positions on the  $\beta - (U - B)_0$  diagram. Corrections for rotation should be applied, for example, in determining any evolutionary differences between the central and outer parts of associations.

It is suggested that a colour index similar to Borgman's  $(Q - P)_0$  would provide a rapid method of determining the ages of faint field stars, since rotational velocities would not be required. For bright field stars, more accurate ages could be determined by averaging the logarithms of the ages deduced from the two methods, because the  $(Q - P)_0 - (U - B)_0$  age diagram is reversed with respect to the  $\beta - (U - B)_0$  age diagram corrected for rotational velocity, and hence any error in  $(U - B)_0$  would have only a small effect on this average.

The calibration of absolute magnitudes from Balmer line intensities given in Chapter 5 is unsatisfactory, since it is based on only two clusters. Further measures of  $\beta$  are required to determine the dependence on age of the relation between  $M_v$  and  $\beta$ . Suitable nearby clusters for investigation would be IC4665 and M34 for which UBV photometry is already available. In the case of associations, the difficulties in determining membership are much more serious. The application of a general correction for rotation awaits the solution of the problem of the inclinations of field stars.

The survey of methods of determining rotational velocities in current use shows that many are subject to systematic errors. In particular, for accurate work the Stark broadening should be taken into account for the helium lines, and several lines should be measured for each star to reduce the effect of blends. Rotational velocities determinations may be extended to fainter B-type stars by making use of the Balmer lines, provided that emission-line stars are excluded.

Rapid and accurate spectral classification of B-type stars is possible on low dispersion objective prism plates. The only plate calibration required is that for the size of the Balmer discontinuity, and this is best provided from photoelectric measures of about 15 stars on each plate.

The discussion on the stars with weak helium lines in Chapter 5 raises the question of the validity of spectral classification by line ratios. McNamara and Larsson (1962) observed that the relative intensities of MgII 4481 and HeI 4471 for HD 37807 in the Orion association give a spectral type B8, while UBV photometry indicates a spectral type B3. If the explanation that such stars are generally rapidly rotating pole-on stars is correct, other lines ratios will be affected in a similar way. Discrepancies between spectral classification by line ratios and classification by UBV photometry would thus be expected for all rapidly rotating pole-on stars.

ACKNOWLEDGEMENTS

This work has been carried out under the supervision of Professor H.A. Brück and Dr. V.C. Reddish, to whom I am very grateful for guidance and helpful suggestions.

My thanks are due to various members of the staff of the Royal Observatory, Edinburgh for assistance in obtaining the plates used in this investigation. I am particularly indebted to Mr. J. Harris for considerable help in aligning the spectrograph of the 36-inch telescope.

REFERENCES

- Abt, H.A., and Hunter, J.H., 1962. Ap. J., 136, 381.
- Allen, C.W., 1955. Astrophysical Quantities, University of London.
- Babcock, H.W., 1960. Stellar Atmospheres, University of Chicago.
- Baker, E.A., 1949. Publ. Royal Obs. Edinburgh, Vol. 1, No. 2.
- Bappu, M.K.V., et al., 1962. M. N., 123, 521.
- Barbier, D., 1962. J. O., 45, 57.
- Berger, J., 1956. J. O., 39, 148.
- Berger, J., 1962. Ann. d'Astrophys., 25, 77.
- Bertiau, F.C., 1958. Ap. J., 128, 533.
- Bidelman, W.P., 1943. Ap. J., 98, 61.
- Blaauw, A., 1956. Ap. J., 123, 408.
- Borgman, J., 1960. B. A. N., 15, 255.
- Butler, H.E., and Seddon, H., 1959. Publ. Royal Obs. Edinburgh, Vol. 2, No. 5.
- Chalonge, D., and Divan, L., 1952. Ann. d'Astrophys., 15, 201.
- Crawford, D.L., 1958. Ap. J., 128, 185.
- Crawford, D.L., 1960. Ap. J., 132, 66.
- Crawford, D.L., 1961. Ap. J., 133, 860.
- Crawford, D.L., 1963a. Ap. J., 137, 523.
- Crawford, D.L., 1963b. Ap. J., 137, 530.
- Eggen, O.J., 1963. A. J., 68, 697.
- Elvey, C.T., 1930. Ap. J., 71, 221.

- Flather, E., and Osterbrock, D.E., 1960. Ap. J., 132, 18.
- Hallam, K., 1959. Doctoral thesis, University of Wisconsin.
- Hardie, R.H., and Crawford, D.L., 1961. Ap. J., 133, 843.
- Harris, D.L., 1955. Ap. J., 121, 554.
- Harris, D.L., 1956. Ap. J., 123, 371.
- Heckmann, O., and Lübeck, K., 1956. Zs. f. Ap., 40, 1.
- Hiltner, W.A., 1956. Ap. J. Suppl., 2, 389.
- Hoerner, S. von, 1957. Zs. f. Ap., 42, 273.
- Huang, Su-Shu, 1953. Ap. J., 118, 285.
- Johnson, H.L., 1955. Ann. d'Astrophys., 18, 292.
- Johnson, H.L., 1958. Lowell Obs. Bull., 4, 37.
- Johnson, H.L., 1960. Lowell Obs. Bull., 5, 17.
- Johnson, H.L., and Morgan, W.W., 1953. Ap. J., 117, 313.
- Jones, D.H.P., 1960. M. N., 120, 43.
- Kaler, J., 1962. Zs. f. Ap., 56, 150.
- Ljunggren, B., and Oja, T., 1961. Ann. Uppsala Obs., Vol. 4, No. 10.
- Malmquist, K.G., Ljunggren, B., and Oja, T., 1960. Ann. Uppsala Obs.,  
Vol. 4, No. 8.
- McNamara, D.H., 1962. Publ. A. S. P., 74, 416.
- McNamara, D.H., 1963. Ap. J. 137, 316.
- McNamara, D.H., and Larsson, H.J., 1962. Ap. J., 135, 748.
- Merrill, P.W., and Burwell, C.G., 1933. Ap. J., 78, 87.

- Morgan, W.W., Keenan, P.C., and Kellman, E., 1943. An Atlas of Stellar Spectra, University of Chicago.
- Mitchell, R.I., 1960. Ap. J., 132, 68.
- Osawa, K., 1959. Ap. J., 130, 159.
- Petrie, R.M., 1952. Publ. Dom. Ap. Obs., 9, 251.
- Petrie, R.M., 1958. M.N., 118, 80.
- Pilowski, K., 1950. Zs. f. Ap., 27, 193.
- Schlesinger, F., 1909. Publ. Allegheny Obs., 1, 134.
- Shajn, G., and Struve, O., 1929. M. N., 89, 222.
- Sharpless, S., 1952. Ap. J., 116, 251.
- Sharpless, S., 1954. Ap. J., 119, 200.
- Sharpless, S., 1962. Ap. J., 136, 767.
- Sinnerstad, U., 1961. Ann. Stockholm Obs., Vol. 22, No. 2.
- Slettebak, A., 1949. Ap. J., 110, 498.
- Slettebak, A., 1954. Ap. J., 119, 146.
- Slettebak, A., 1963. Ap. J., 138, 118.
- Slettebak, A., and Howard, R.F., 1955. Ap. J., 121, 102.
- Strömberg, B., 1952. A. J., 57, 200.
- Su-Shu Huang, and Struve, O., 1956. Ap. J., 123, 231.
- Struve, O., 1929. Ap. J., 70, 237.
- Sweet, P.A., and Roy, A.E., 1953. M. N., 113, 701.
- Treanor, P.J., S.J., 1960. M. N., 121, 503.



Unsöld, A., 1955. Physik der Sternatmosphären, p. 478, Berlin.

Vitense, E., 1951. Zs. f. Ap., 29, 73.

Williams, E.G., 1936. Ap. J., 83, 305.

Note. Most of the discussion given in Chapters 2 and 5 was published in 1963 in "Publications of the Royal Observatory, Edinburgh", Vol. 3, No. 4.